Tatiana dos Reis Martins

Licenciada em Biotecnologia

Microencapsulation of antitubercular drugs in a matrix of partially hydrolyzed guar gum, for application in tuberculosis treatment

Dissertação para obtenção do Grau de Mestre em Bioquímica para a Saúde

Orientadora: Dr.ª Ana Margarida Grenha, Professora Auxiliar, Universidade do Algarve

Dezembro, 2015

Tatiana dos Reis Martins

Licenciada em Biotecnologia

Microencapsulation of antitubercular drugs in a matrix of partially hydrolyzed guar gum, for application in tuberculosis treatment

Dissertação para obtenção do Grau de Mestre em Bioquímica para a Saúde

Orientadora: Dr.ª Ana Margarida Grenha, Professora Auxiliar, Universidade do Algarve

Trabalho de Investigação realizado em: UAlg UNIVERSIDADE DO ALGARVE

Júri:

Presidente: Prof. Doutor: Pedro Matias
Arguente: Prof. Doutora: Manuela Gaspar
Vogal: Prof. Doutora: Margarida Archer

ITQB, Oeiras

Dezembro, 2015

Microencapsulation of antitubercular drugs in a matrix of partially hydrolyzed guar gum, for application in tuberculosis treatment

Declaração de autoria de trabalho:

Declaro ser a autora deste trabalho, que é original e inédito. Autores e trabalhos consultados estão devidamente citados no texto e constam da lista de referências incluída no documento.

Tatiana dos Reis Martins

Agradecimentos

Antes de mais gostaria de agradecer à minha Orientadora, a Professora Doutora Ana Grenha pelo seu acompanhamento, pelas reuniões, pelas críticas construtivas, pelos ensinamentos e paciência acima de tudo.

Quero expressar também os meus agradecimentos à Professora Doutora Leonor Faleiro, que representou para mim um papel de co-orientadora, pois representou um apoio importante na obtenção das estirpes bacterianas, na sua manipulação e na discussão de vários ensaios com bactérias quer preliminares quer efetivos, de forma a obter resultados representativos e robustos.

Gostaria de agradecer ao Professor Doutor João Lourenço que ajudou a determinar a estabilidade das micropartículas por Difração de Raios-X e apoiou bastante no tratamento e discussão destes dados.

Gostaria de agradecer à Professora Doutora Manuela Gaspar, por autorizar a utilização do picnómetro da FFUL, com o fim de determinar a densidade real das micropartículas.

Quero agradecer também, à técnica Cláudia Florindo que manipulou o microscópio de Epiflurescência e permitiu a obtenção de fotografias de fluorescência e contraste de ambas as estirpes de interesse, após várias tentativas até encontrarmos uma imagem decente, requerendo bastante paciência. E também à técnica Liseta pela sua simpatia, boa disposição e apoio.

Os maiores agradecimentos a todos os meus colegas do laboratório 2.22 (incluindo os alunos do Professor Mathias, o Miquel e o Joaquin) e colegas do 2.21 (que em parte foi como uma segunda “casa”), à Rita Nascimento do laboratório 3.30, à Catarina Afonso do CCMAR, quer pelo apoio, pela instrução, pela boa disposição, pelo companheirismo ao longo da minha breve estadia neste laboratório.

Por fim, devo um agradecimento à minha família pelo apoio, pela guarida e pela força que me permitiu avançar até este ponto.

Aos meus grandes amigos que estiveram presentes em variados momentos que me proporcionaram momentos de alegria, que me aconselharam e de que de alguma forma me acompanharam nesta viagem com altos e baixos. O meu maior obrigado!

Abstract

Tuberculosis (TB), despite being a completely curable disease, has reemerged due to drug resistance and deadly synergism with HIV infection, which limit the success of its management. Lung tuberculosis is the main manifestation of TB. Thus, exploring the inhalable route for a local delivery of antitubercular drugs seems a promising therapeutic approach. Partially hydrolyzed guar gum (PHGG) is a strong candidate as matrix material for antitubercular drug carriers. This is mainly due to its affinity for macrophages, the hosts of mycobacteria, which is mediated by the binding of sugar units to macrophage surface receptors. In this work, PHGG-based microparticle formulations were produced by spray-drying, evaluated for cristallinity pattern (X-ray diffraction) and ability for drug association, and *in vitro* drug release profiles were determined. The cytotoxicity of microparticles was also evaluated (MTT and LDH release assays). Additionally, the therapeutic effect of drug-loaded microparticles was evaluated *in vitro* on macrophage-like cells infected with mycobacteria strains. The results showed that microparticles exhibited suitable properties for pulmonary delivery (aerodynamic diameter between 1 and 3 μm). A favorable cytotoxic profile was evidenced, as no overt toxicity was detected in representative respiratory cell lines (A549 and Calu-3 cells), although a mild toxic effect was observed in macrophage-like cells. The *in vitro* response of infected macrophages to drug-loaded PHGG microparticles was considered promising, as only 20% of mycobacteria remained viable upon a single treatment with microparticles. This thesis addresses macrophages as therapeutic target, unraveling the unique role of polysaccharides on pulmonary drug delivery in the ambit of tuberculosis therapy.

Key words: Guar gum, macrophage targeting, microparticles, spray-drying, tuberculosis therapy.

Resumo

Tuberculose (TB), apesar de ser uma doença totalmente curável, tem reemergido devido à resistência a fármacos e ao sinergismo fatal com o VIH, o que limitou o sucesso de sua gestão. Tuberculose pulmonar é a principal manifestação da TB, assim, explorar a rota inalável para uma entrega local de fármacos antituberculares parece ser uma abordagem terapêutica promissora. Goma guar parcialmente hidrolisada (PHGG) é um forte candidato, como material matriz transportadora de fármacos antituberculares. Isto principalmente devido à sua afinidade para os macrófagos, os hospedeiros de micobactérias, mediada pela ligação de unidades de açúcar aos recetores de superfície de macrófagos. Neste trabalho, as formulações de micropartículas baseadas na matriz de PHGG foram produzidas por atomização, os seus padrões de cristalinidade (difração de raios-X) foram avaliados, a sua capacidade de associação de fármacos e o perfil de libertação *in vitro* de fármacos foram determinados. A citotoxidade das micropartículas foi também avaliada (ensaios de MTT e libertação de LDH). Além disso, o efeito terapêutico de micropartículas com fármacos, foi avaliado *in vitro* em células similares a macrófagos infetadas com estirpes micobacterianas. Os resultados mostraram que as micropartículas exibiram propriedades adequadas para entrega pulmonar (diâmetro aerodinâmico entre 1 e 3 μm). Evidenciaram um perfil citotóxico favorável, na ausência de citotoxicidade detectável nas linhas de células respiratórias representativa (A549 e Calu-3 células), apesar de um ligeiro efeito tóxico observado em células similares a macrófagos. A resposta *in vitro* de células similares a macrófagos infetadas por micropartículas de PHGG com fármacos antituberculares foi considerada promissora, uma vez que a viabilidade micobacteriana de 20% foi obtida após um único tratamento com micropartículas. Esta tese aborda os macrófagos como alvo terapêutico, desvendar o papel único de polissacarídeos na entrega da droga pulmonar no âmbito da terapia da tuberculose.

Palavras-chave: Atomização, goma guar, micropartículas, terapêutica da tuberculose, vetorização para os macrófagos.

Contents

Index of figures

Index of tables

Abbreviations list

A549 cell line – Adenocarcinomic human alveolar basal epithelial cell line

Abs – Absorbance

AE – Association efficiency

AG – Arabinogactan

AIDS – Immunodeficiency syndrome

AM – Alveolar macrophage

ANOVA – Analysis of variance

ATTC – American Type Culture Collection

BCG – Bacillus Calmette-Guérin

Ca^{2+} – Calcium

Calu-3 cell line – Adenocarcinomic human bronchial epithelial cell line

CM – Culture medium

CO_2 – Carbon dioxide

CRX – Chest radiography with X-rays

CuKα – Potassium calcium alpha

CYP4A4 – Cytochrome involved in human liver metabolism

d_{ae} – Aerodynamic diameter

DMEM – Dulbecco's modified eagle medium

DOTS – Observed treatment and short-course drug therapy

EDTA – Ethylenediamine tetraacetic acid

EMB – Ethambutol

FBS – Fetal bovine serum

FDA – Food and drug administration

FESEM – Field emission scanning electron microscopy

GRAS – Generally recognized as safe

HCl – Hydrochloric acid

HIV – Human immunodeficiency virus

IL – Interleukin

INH – Isoniazid

INT – Iodonitrotetrazolium

LAM – Lipoarabinomannan

LC – Loading Capacity

LDH – Lactate dehydrogenase enzyme

M – Medium

M7H9 – Middlebrook's 7H9 broth base

MA – Mycolic acid

Man – Mannitol

ManLAMs – Lipoarabinomannan capped with mannose residues

MDR – Multidrug resistance tuberculosis

MIC – Minimum inhibitory concentration

MTB – *Mycobacterium tuberculosis*

MOI – Multiplicity of infection

MPs – Microparticles

MTBC – *Mycobacterium tuberculosis* Complex

MTT – 3-(4,5-Dimethylthiazol-2-yl)-2,5-diphenyltetrazolium salt

NAD(P)H – Reduced nicotinamide adenine dinucleotide (phosphate)

NAAT – Automated nucleic acid amplification test

Ni – Nickel

NK cells – Natural killer cells

OADC – oleic acid, albumin, dextrose and catalase supplement

OD – Optical density

PBS – Phosphate-buffered saline

PG – Peptidoglycan

PHGG – Partially hydrolyzed guar gum

PILAM – Lipoarabinomannan capped with phosphoinositol

PIM – Phosphatidylinositol mannoside

PMA – Phorbol myristate acetate

PZA – Pyrazinamide

RIF – Rifampicin

RFB – Rifabutin

RPMI – Roswell Park Memorial Institute medium

S – SDS 2%

SD – Spray-dried

SDS – Sodium dodecyl sulfate

SEM – Standart error of the mean

TB – Tuberculosis

THP-1 cell line – Human monocytic cell line

UV-Vis – Ultraviolet visible spectroscopy

XDR-TB – Extensively drug-resistant tuberculosis

XRD – X-rays diffraction

WHO – World Health Organization

Chapter I - Introduction

1.1. Historical perspective and epidemiology of tuberculosis

Tuberculosis (TB) is an infectious disease caused by *Mycobacterium tuberculosis* (MTB). It has been reported since the ancient Greco-Roman and Egyptian civilizations, for about 3.000 years BC [1, 2]. The disease was initially reported as consumption or phthisis, which means decline. Laennec, the inventor of the stethoscope, discovered that tubercles, characteristic lesions found in the lungs, were also found in other locations, such as the spine and lymph glands. Therefore, he realized that this disease occurred throughout the body. Curiously he died of tuberculosis after publishing his research [3].

Although MTB had been always present, it was regarded as an unimportant pathogen to man, until a tuberculosis epidemic was unleashed in result of urbanization and industrialization around the globe [2, 3]. Known as the "great white plague", TB was the main death cause in Europe and in United States of America, in the mid-1700's and 1800's [1, 2]. In 1882, Robert Koch, a German physician presented his research on the tubercle bacillus, which turned out to be crucial in the understanding of the most significant infectious disease of the period. Later on, in 1905, his work on tuberculosis earned him a Nobel Prize [3, 4].

With the establishment of the World Health Organization (WHO), tuberculosis was recognized as a top priority. Therefore, as an effort towards its control, the Bacillus Calmette-Guérin (BCG) vaccine and antibiotic drugs were developed. The vaccine is based on the attenuated virulence of *M.bovis* and still remains one of the most used worldwide.

Another important mark was the discovery of streptomycin by Waksman and Schatz, but the antibiotic quickly showed several problems concerning its price, side effects and the developed resistance. Cheaper synthetic compounds like aminosalicylic acid and isoniazid (INH) were produced, but one major problem remained, as the treatment required the hospitalization for 12 to 18 months. The evolution of therapy has dictated a reduction in the treatment period to six months, making patient compliance less complicated, but still not satisfactory [1, 3].

Nowadays, TB remains a major global health burden, continuously spreading and infecting millions of people each year [5, 6]. TB is considered the second most deadly infectious disease worldwide, after the human immunodeficiency virus (HIV). In 2013 the reports estimated that there were 9.0 million new TB cases and 1.5 million TB deaths (0.4 million among HIV positive people).

The greatest number of cases in 2013 occurred in Asia (56%) and Africa (29%), while a smaller number of cases occurred in the Eastern Mediterranean Region (8%), European Region (4%) and America (3%). One of the greatest problems related with TB disease relies on the co-infection with HIV. The proportion of co-infection cases revealed to be higher in Africa, with more than 50% of the cases occurring in the Southern African Region (Figure 1.1) [7].

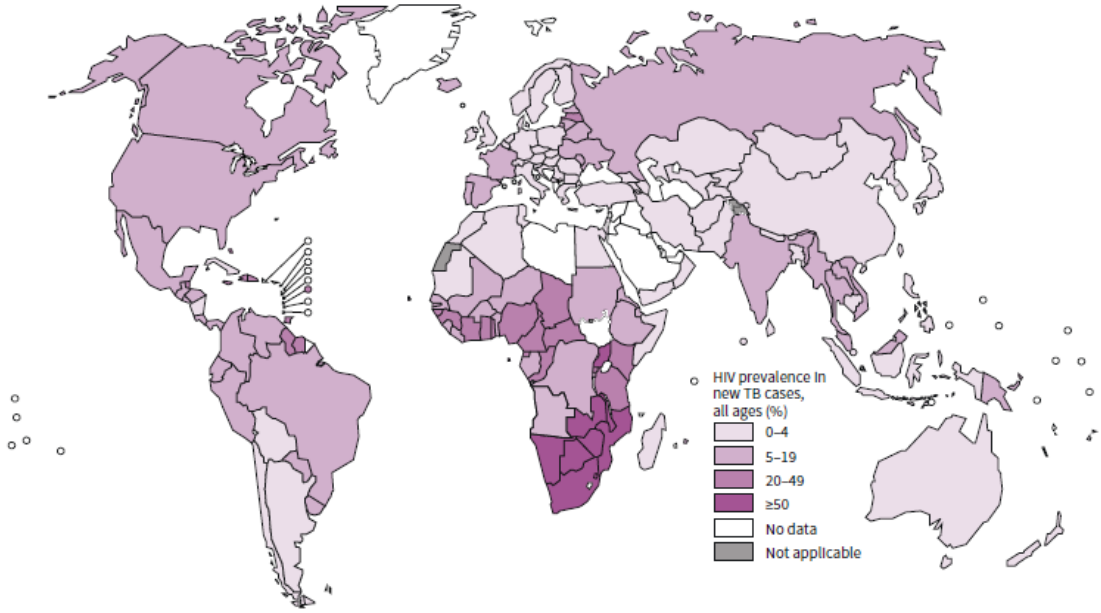

Figure 1.1 – Estimated co-infected TB with HIV cases all over the world.

Reprinted from: WHO, World Heal. Organ., 2014 [7].

The current epidemic is being maintained and sustained in the presence of immunosuppressive conditions like diabetes, alcoholism, malnutrition, chronic lung disease and HIV [5, 8]. It is well established that the immune system is compromised by HIV infection, which will predispose for the development of TB. As result of HIV infection, $CD4^+$ T-lymphocytes decrease, leading consequently to the acquired immunodeficiency syndrome (AIDS). Therefore, the risk of acquiring TB in a compromised individual is 30%. In contrast, a healthy individual has only a 3% probability of contracting TB. The infection caused by MTB was reported as being the most lethal and opportunist pathogenesis when is found in a synergic co-infection with HIV [4].

1.2. Pathogenesis of tuberculosis

TB is a respiratory contagious bacterial infection, occurring when an uninfected person inhales an infected droplet which was produced from an individual with active TB [5, 6]. The content of this droplet then deposits at the terminal airways or pulmonary alveolus [2, 5, 11, 12]. The infecting mycobacteria colonize primarily the lungs (pulmonary TB), but they can disseminate to extra-pulmonary areas of the organism, mainly the circulatory and nervous systems [5, 9]. The resulting symptoms of pulmonary TB are chronic bloody coughs, night sweats and weight loss. Extra-pulmonary TB can manifest as pericarditis, meningitis, or spinal TB [12].

Once inside the pulmonary alveoli, the bacilli will interact with dendritic cells, alveolar macrophages (AMs) and pulmonary epithelial cells. Capable of invading any of these, their preference is to be hosted by AMs [13]. AM pathogen recognition receptors recognize pathogen-associated molecules pattern, mediating phagocytosis, a normal innate immune response [12, 13]. This recognition can be made by surface receptors, namely complement

receptors, or through recognition of mannose residues, specifically mannose-capped lipoarabinomannan (LAM) through mannose receptors. This route will direct the bacteria to the phagosome, leading to its arrest [13]. The infected cells release pro-inflammatory cytokines leading to the recruitment of mononuclear cells. After this event, the antigens are presented to specific T-lymphocytes which become activated as well. Cytokines IL-12 and IL-18 are secreted from infected cells and induce Natural Killer (NK) cell activity; thereby NK cells produce Interferon-γ leading to the activation of other macrophages, which results in the production of tumor necrosis factor-α [10, 11]. In a posterior phase, macrophages, lymphocytes and extracellular matrix proteins surround the infected macrophages in a structure called granuloma [12]. Within this structure MTB can be contained, leading to the formation of another structure called tubercle, resulting in latent TB infection, characterized by the permanence of the pathogen in a dormant state at the arrested site, for indefinite time. However, if the host immune system is compromised, the above described response is not adequate and the pathogen will systematically multiply, resulting in reactivated TB [11, 12, 14]. The final outcome is thus fully dependent on the immunological response given by the affected individual [12, 14].

Reports by Yuk and Jo (2014) and Welin (2010) indicate that MTB might be phagocytized by AMs and eliminated via apoptosis or autophagy. If the bacteria gets arrested, but not eradicated, the disease gets in a latent assymptomatic state. Latent TB infection is developed by 90-95% of infected individuals. In the case that MTB surpasses the host immune system, replication inside AM occurs followed by dissemination through the lungs, which results in the development of active TB (Figure 1.2). A progression of latent TB infection may however occur in case of simultaneous HIV infection, prescription with immunosuppressive drugs, or through re-infection, for example [12, 15]. The eradication of mycobacteria implies the maturation of the phagosome, leading to “classical activation” response of the macrophage, implying calcium mobilization, followed by a respiratory burst featuring the formation of free radicals, resulting in an acidification of the phagosome and therefore the digestion and destruction of the foreign material. In the case of an “alternative activation” the activated macrophages show different gene regulation resulting in different expression of cell-surface pathogen recognition receptors, production of other cytokines and chemokines. In addition, alternatively-activated macrophages produce reduced amount of nitric monoxide. Importantly, this kind of activation is reported to support mycobacterial growth rather than inhibition [16].

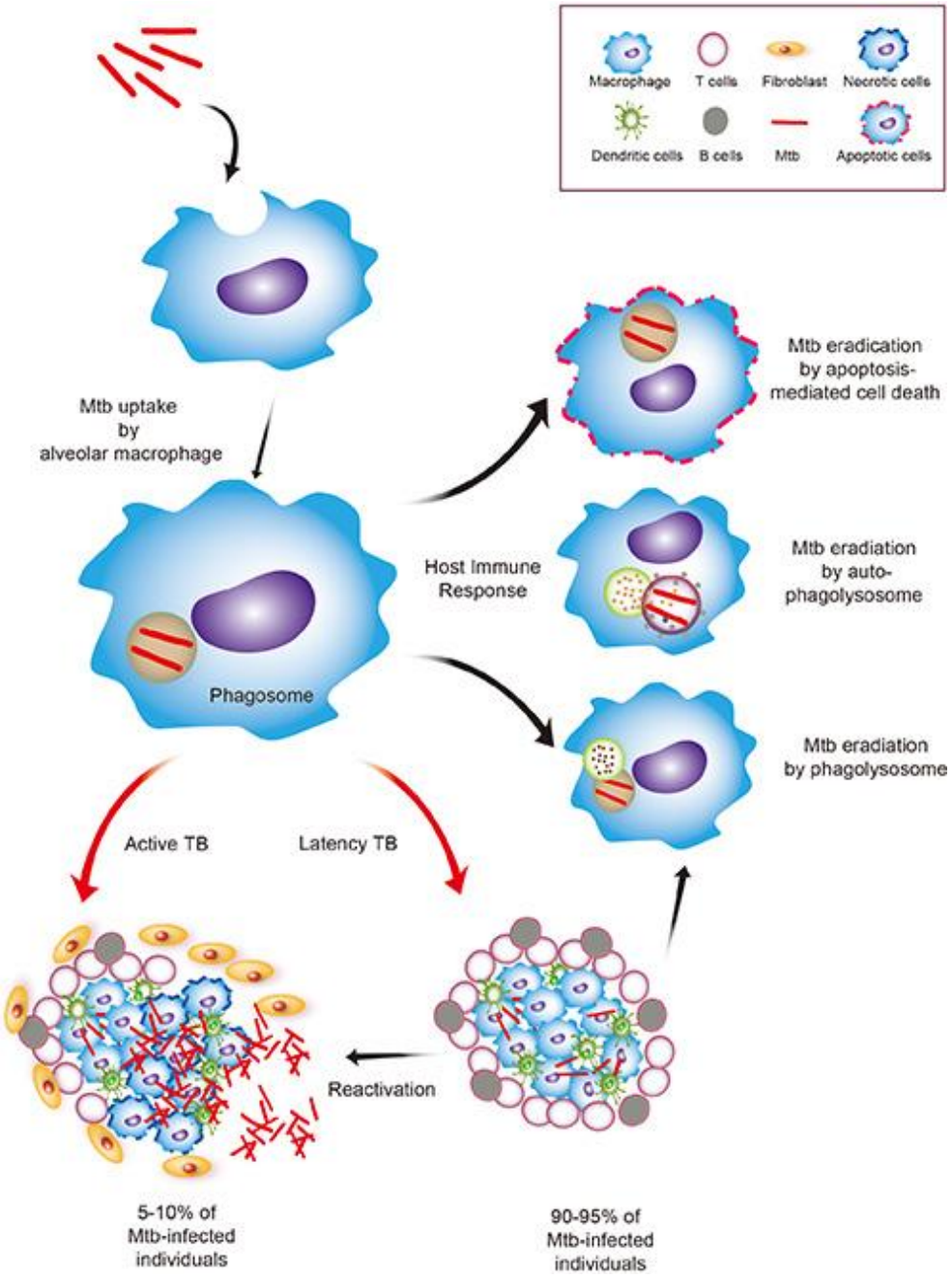

Figure 1.2 – Schematic diagram of the events occurring on macrophages infected with MTB. In 90-95% of the cases the disease stays arrested in the latent form, which is asymptomatic. In 5-10% of cases, MTB replicates inside the macrophage and the disease stays active, developing typical symptoms.

Reprinted from: Yuk and Jo, Clin. Exp. Vaccine Res., 2014 [15].

1.3. *Mycobacterium spp*.

Mycobacteria belong to the *Actinomycetales* order, and *Mycobacteriaceae* family. The following taxonomy is based on three criteria: resistance to alcohol-acid decolourisation; mycolic acid synthesis and percentage of cytosine and guanine [1, 16]. *Mycobacterium* genus includes the *M. tuberculosis* complex (MTBC), the *M. avium* complex and other saprophytic mycobacteria species [1]. The MTBC includes several related species*: M. tuberculosis M. bovis*, *M. africanum*,

M. microti, *M. pinnipedii*, *M. caprae* and *M. cannetti* [1, 11]. Kazda [17] classified mycobacteria from a pathogenic point of view, into three groups: strictly pathogenic, potentially pathogenic and rarely pathogenic or saprophytic. All MTBC members are strictly pathogens, causing tuberculosis, and are closely similar from a genetic point of view. For example, the genome of MTB shows only <0.05% difference with *M. bovis* [11, 12].

MTB are rod-shaped mycobacteria with a length of 1-4 μm and about 0.5 μm of diameter. They are classified as Gram positive, although poorly staining crystal violet. The complex cell wall composition gives resistance to decolourisation by acid during staining procedures. For this reason they are termed acid fast bacilli [17]. MTB is an intracellular pathogen that survives inside the phagosomes of macrophages preventing their maturation to phagolysosomes. It is a strict aerobic and replicates very slowly, with a doubling time roughly 24 hours [1, 10, 17]. The distinction between fast and slow growing species is determined based on whether a visible colony grows in less or more than seven days [1].

The knowledge and understanding achieved on survival mechanisms used by mycobacteria inside the organism cells might be useful for the elimination of these pathogens. The research assays made in this thesis involve two important strains that belong to the *Mycobacterium* genus, *M. bovis* and *M. smegmatis*, which characteristics are detailed below.

1.3.1. *Mycobacterium bovis*

M. bovis comprises slow-growing mycobacteria that have a doubling time of 18-20 hours. The slow growing is mainly related with the complexity of the cell wall and the high nutritional demands [18]. *M. bovis* is the main responsible pathogen in livestock and wild animals, causing bovine tuberculosis. This might contaminate humans as well, causing a type of tuberculosis that is indistinguishable from the one caused by *M. tuberculosis* [11, 19]. The contamination of humans has been usually mediated by ingestion of non-pasteurized cow's milk [9].

BCG became an attenuated strain of *M. bovis* and was first administered to humans as a vaccine in 1921. It contains posterior deletions with the loss of a 10 Kb region of deletion 1 from the DNA, that has the gene ESAT-6, thus resulting in an attenuation of its virulence [1, 11]. BCG is the most used vaccine worldwide, presenting advantages, such as low production cost, safety and stability, long immunization protection provided by a single dose and possibility of administration to newborns [20].

1.3.2. *Mycobacterium smegmatis*

M. smegmatis was isolated for the first time by Alvarez and Travel, in 1885 [20]. This is a fast-growing strain, which has a doubling time of 4-6 hours, but besides this different characteristic, it shows some similar features with the pathogenic *M. tuberculosis* [11, 21].

M. smegmatis is a saprophytic strain, classified as non-pathogenic [1, 11]. As it lacks the pathogenic properties of *M. tuberculosis*, it is consequently not suitable for virulence studies, but is largely used for physiological studies [9].

The essential difference between non-pathogenic and pathogenic strains is that during phagocytosis, the non-pathogenic strain gets rapidly destroyed by proteases from the resulting arrest in phagosomes of infected host; while the expressed antigens are quickly absorbed, inducing a strong immune response [20]. Although *M. smegmatis* is widely considered to be non-pathogenic, some data report that it behaves as a pathogen capable of manipulating the system [22].

1.3.3. Mycobacterial cell wall

The mycobacterial cell wall has unique characteristics and some of its components are responsible for the inherent resistance to several drugs. Mycolic acid is responsible for conferring resistance to the previously mentioned alcohol-acid decolourisation, as well as to chemical agents and antibiotics [17]. Figure 1.3 illustrates the composition of MTB cell wall, where long chains of fatty acids defined as mycolic acids are linked to arabinogalactan, which is covalently linked to the peptidoglycan, forming the MA-AG-PG complex. This complex is insoluble and considered an important core of the mycobacterial cell wall [4, 22]. PG is constituted of alternating units of *N*-acetyl glucosamine and a *N*-glycolylated muramic acid [4]. Lipoarabinomannan (LAM) and phosphatidylinositol mannoside (PIM), a biosynthetic precursor of LAM, are lipoglycans non-covalently attached to the cell wall through their glycosylphosphatidylinositol anchors [10, 22].

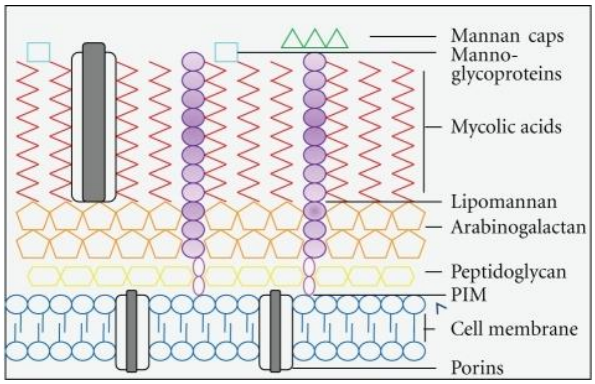

Figure 1.3 – Representative scheme of *M. tuberculosis* cell wall structure. The figure shows the major components of the cell wall and their distribution. Schematic complex MA-AG-PG, mannose-capped glycoproteins, lipomannan and mannoglycoproteins are displayed.

Reprinted from: J. Kleinnijenhuis *et al*, Clin. Dev. Immunol, 2011 [24].

Both phosphatidylinositol derivatives PIM and LAM resemble typical mammalian phospahtidylinositol, which generate membrane traffic-regulating species. PIM has an inositol ring glycosylated with mannose; its role is to stimulate the fusion between phagosomes and early endosomes [25]. LAM acts as a virulence factor of MTB, being responsible for the phagosome maturation arrest, inhibiting the increase of cytosolic $[Ca^{2+}]$. This blocks the successive steps of phagolysosome maturation and acidification [26], affects T-cell activation,

avoids reactive species of oxygen and reactive nitrogen intermediates to act through antimicrobial mechanisms, and inhibits several transduction cascades regulated by protein kinase C [4, 10]. In slow-growing pathogenic mycobacteria, such as MTB, these LAMs are capped with mannose residues and are denominated as ManLAMs, whereas fast-growing such *as M. smegmatis*, have phosphoinositol-capped LAMs referred as PILAMs [10, 22].
These phosphatidylinositols display several immunomodulatory proprieties by interaction with several receptors of the immune system. PIMs and ManLAMs are recognized by C-type lectins and the macrophage mannose receptors [27].

1.4. Diagnosis and treatment of tuberculosis

Diagnostic methods for TB include chest radiography (CRX), sputum smear microscopy, tuberculin skin test, interferon-γ release assay, line probe assay and automated nucleic acid amplification tests (NAATs), among others [10, 25]. CRX is useful to detect the presence of fibrous scarring of the lung parenchyma, and other pulmonary lesions, indicating if tuberculosis is already established and/or active. Computed tomography is an additional imaging modality to study TB, useful after an inconclusive CRX screening [29]. The nucleic acid amplification tests (NAATs) are based on amplifying regions specific to the MTBC.

All the mentioned detection methods have advantages and inherent limitations; as described in Table 1.1.

Table 1.1 – Tuberculosis diagnostic methods in use, recently approved by WHO.

Method	Use	Advantages	Limitations
Smear microscopy	Rapid tubercle bacilli detection	Moderate training, low price	Low sensitivity
Chest radiography	Pulmonary TB detection	Indications and use not restricted to TB	Low specificity and sensitivity, trained clinician
Tuberculin skin Test	Detection of *M. Tuberculosis*	Extensive clinical and published experience	Low sensitivity in immunocompromised patients, positive for vaccinated BCG persons
γ-Interferon release assay	Detection of *M. tuberculosis* infection	Highly specific for *M. tuberculosis*	Trained personnel, poor sensitivity
Automated nucleic acid amplification tests (NAATs)	Pulmonary TB detection	High sensitivity, detection of mutations in MDR-TB strains	Moderately trained persons and equipment, laborious and possible cross-contamination
Line probe assay	TB detection and drug susceptibility testing	Short analysis time	Labor intensive, potential for cross-contamination, requires much training

Adapted from: Kanwar, Underst. Tuberc. - Glob. Exp. Innov. Approaches to Diagnosis, 2012 [28].

The conventional therapeutic approach of tuberculosis is based on oral antibiotherapy. WHO recommends an oral co-administration regimen of four first-line antibiotics: isoniazid (INH), rifampicin (RIF), ethambutol (EMB) and pyrazinamide (PZA). Monotherapy is not recommended for TB. Instead, a correct drug association, in adequate doses during the time prescribed is a standard measure to avoid bacterial persistence and resistance to antibiotics [27, 28].

Antibiotherapy is administered by Directly Observed Treatment and Short-course drug therapy (DOTS) programs, which ensures compliance on the patience's behalf through their observation [12]. During the initial 2 months the four first-line antibiotics are prescribed, being then reduced to RIF (600 mg or 450 mg daily) and INH (300 mg daily) [4] for the following 4 months. A long prescription is normally associated with compliance issues, and may lead to serious secondary toxic effects provoked by several of these antibiotics. For instance, INH induces hepatotoxicity in humans, which is potentiated when co-administrated with RIF, due to a bigger induction of CYP450 enzymes, and overproduction of toxic hydrazine metabolite [32].

One important factor to be reckoned is the widespread emergence resistance of MTB to the most effective anti-TB drugs [12, 30]. Different mechanisms are assumed to result in the development of drug resistance, but in the case of MTB the main mechanism is attributed to

gene mutations [4]. It is reported that more than 3% of TB patients worldwide are resistant to two of the major first-line anti-TB drugs, INH and RIF, condition referred as multidrug resistance (MDR-TB). About 9% of MDR-TB cases can also show resistance to second-line anti-TB drugs, a condition called extensively drug-resistant TB (XDR-TB). When these conditions are observed, the implemented therapeutic protocols differ from the conventional one, requiring instead at least five drugs which are less strong, showing higher toxicity and being more expensive [3, 30].

1.5. Antitubercular drugs

TB can be effectively treated with the use of first-line drugs, INH, RIF and derivatives such as rifabutin and rifapentin, PZA, EMB and streptomycin. However, this therapy can fail for several reasons. As previously mentioned, the emergence of drug resistant mycobacteria is one crucial challenge regarding tuberculosis therapy, demanding the use of second-line antitubercular drugs (fluoroquinolones, aminoglycosides, cycloserines and ethionamides/prothionamides) [34].

In this thesis two first-line drugs were used, INH and rifabutin. Their main characteristics are described below.

1.5.1. Isoniazid (INH)

INH, which chemically is pyridine-4-caboxylic acid hydrazide (Figure 1.4), is denoted with the formula $C_6H_7N_3O$. It has a molecular weight of 137.14 g/mol and is highly soluble in water (125 mg/mL) [31]. This antitubercular agent is a hydrophilic pro-drug that is activated by the gene *katG*, encoding the catalase peroxidase enzyme which causes a lethal effect on intracellular pathogens. INH is only active against growing tubercle bacilli. Activated INH inhibits the synthesis of mycolic acids by inhibition of NADH-dependent enoyl-acyl carrier protein reductase encoded by the gene *inhA* [34].

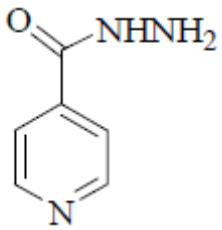

Figure 1.4 – Chemical structure of isoniazid.

It has been reported that mutations in the genes *katG*, *inhA* and *ahpC* are related with INH resistance. MTB is normally susceptible to INH (MIC 0.02-0.2 μg/mL), however there are isolates that might lose their protein *katG* activity, interrupting the bacteriostatic action onto the

bacilli. Ser315Thr is the most common mutation, leading to the inactivation of catalase peroxidase enzyme. A high INH resistance has been observed in other mycobacterium strains, such as *M.smegmatis* and *M.bovis*, with MIC values ranging between 0.2 and 256 μg/mL. This high resistance values are mainly explained by *katG* mutations [32, 33]. *InhA* mutations are less frequent than *katG* mutations, often resulting in low-level resistance (MIC 0.2-1 μg/mL). If for instance, a resistant strain harbors both mutations, this will result in a synergetic outcome and higher levels of INH resistance. *AhpC* gene codes for an alkyl hydroperoxidase reductase, implying protection against reactive oxygen and nitrogen intermediates, avoiding the antimicrobial action due to the interruption of the defense macrophage mechanism [34].

1.5.2. Rifabutin (RFB)

Rifamycins (rifampicin, RFB and rifapentin) belong to the same family, represented by their unique molecular architecture composed by aromatic groups linked by aliphatic chains in non-adjacent positions. Figure 1.5 represents the specific chemical structure of RFB [36].

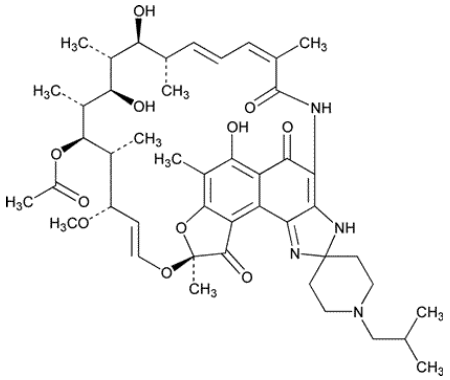

Figure 1.5 – Chemical structure of rifabutin.

RFB, has the molecular formula of $C_{46}H_{62}N_4O_{11}$, a molecular weight of 847.005 g/mol and is poorly soluble in water (0.19 mg/mL) [31, 37]. It is a first-line antitubercular drug particularly used in patients co-infected with AIDS, due to its lack of interaction with retroviral drugs [38]. Its mechanism of action is based on binding to the β-subunit of RNA polymerase (*rpoB*), inhibiting the transcription activity and leading to the organism death. An important advantage of this drug resides in its action on growing and non-growing bacilli, an ability not evidenced by INH, as commented before. Most part of MTB isolates resistant to RIF show mutation in the gene *rpoB*, which translates in a conformational change with low affinity to the drug, consequently leading to resistance [34]. Although RIF is very frequently used in TB therapy, RFB presents longer half-life, lower toxicity outcomes, is active at lower doses than RIF and has equal propensity to trigger drug resistance [38]. Pharmacokinetic and pharmacodynamic data obtained in a mouse

model suggest additional advantages of RFB over RIF, such as minimal induction of CYP3A4/5 and a fast eradication of MTB infection [31]. The only valid disadvantage regarding the use of RFB over RIF is its higher cost [39].

RFB's MIC for MTB susceptible strains is around 0.004 μg/mL, while resistant strains having resistance mutations in gene *rpoB*, show MIC values varying between 0.25 and 16 μg/mL, depending on the mutation [40].

1.6. Pulmonary drug delivery

As mentioned above, the conventional treatment of TB usually involves systemic delivery of antitubercular drugs through the oral route. The major disadvantages related with this conventional approach are the undesirable side effects and toxicity associated to the administered doses. Taking into account that TB is an airborne infection, with a great accumulation of mycobacteria in the lung alveoli and, particularly, in the alveolar macrophages, pulmonary drug delivery could represent a great alternative to reach effective drug concentrations in the alveolar macrophages. With this strategy, lower doses could be administered, as the drugs would be co-localized with the infecting agents [38–40]. This would possibly reduce dose frequency and the duration of treatment, lowering the systemic toxicity, and ultimately improving patient compliance [15, 40].

An effective administration of drugs by the pulmonary route requires the application of carriers, not only because these will provide protection to the encapsulated molecules, but also due to the required characteristics to reach the alveolar region and trigger macrophage uptake. Carriers of size between 1 and 2 μm have been reported to have a maximized probability of phagocytosis by AM [44] and, within the set of available carriers, microparticles (MPs) are those described on most occasions. In MPs, having a low density provides improved dispersibility and lowers the aerodynamic diameter, which can help reaching the alveolar zone and emitting doses from the inhalers [43, 45]. Particle deposition takes place by inertial impaction, sedimentation, and diffusion. Whereas microparticles > 5 μm tend to deposit by impaction in extra thoracic zones, particles with size of 1-5 μm deposit deeper in the lungs reaching the alveoli by inertial impaction and sedimentation, while very small particles of < 1 μm are driven by diffusion, with a high chance to be exhaled [8, 40]. Hence, the aerodynamic diameter of microparticles designed with the purpose of carrying drugs, should range from 1 to 5 μm to guarantee a maximum deposition in the deep lung [44]. The relation between deposition (%) and particle size (μm) is presented in Figure 1.6.

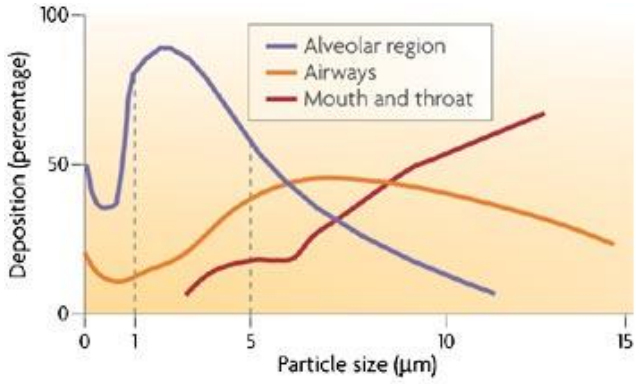

Figure 1.6 –Lung particle deposition pattern according to particle size.

Adapted from: Patton and Byron, Nature Reviews Drug Discovery, 2007 [46].

Although pulmonary drug delivery has been referred very frequently in the ambit of the design of therapeutic approaches for systemic diseases, this route is considered the most appropriate route for the treatment of pulmonary diseases like asthma and chronic obstructive pulmonary disease, and a very promising alternative in the case of lung cancer and tuberculosis [42].

1.7. Polymeric microparticles of partially hydrolyzed guar gum

A multitude of materials are known for their ability to encapsulate, entrap or attach to a matrix, and there are different types of materials of interest in this area. However, there is a limited number of materials certified as “generally recognized as safe” (GRAS) by the FDA and the list is even narrower when regarding materials approved for pharmaceutical applications [47]. Various synthetic and natural polymers revealed to be useful in the formulation of inhalation therapies. Synthetic materials present significant limitations, for instance the generally reported low drug association rates and their high cost. In turn, the selection of natural polymeric materials as matrix components, such as polysaccharides, is frequently observed in drug delivery research. These have been described as the most suitable for this kind of application, owing to their structural flexibility, biodegradability, biocompatibility, hydrophilic character and availability at relatively low prices [5]. These polymers are mainly composed by sugar residues, such as mannose, galactose and fucose. Having these units on their composition offer polysaccharides a great ability to directly target macrophages. As said in section 1.2, macrophages have several surface receptors, one of them being the mannose receptor. This is capable or recognizing units such as those referred above to compose polysaccharides [48]. Therefore, polysaccharides bearing these units might mediate macrophage targeting. Natural polysaccharides can be obtained essentially from three main sources: plant, marine and microbial/animal origin [47]. Because of the above indicated properties of natural polymers, their pharmaceutical applications have been growing in number and variety. In a general manner (not restricting to pharma applications), natural gums have been the most widely used. In the

pharmaceutical field their application is mainly dedicated to tablet production and stabilization of processes [44, 45].

Guar gum is a natural water soluble, nonionic polysaccharide extracted from the endosperm of guar beans of *Cyamopsis tetragonolobus*, a leguminous plant cultivated essentially in India and Pakistan. Chemically, guar gum belongs to the galactomannan family, showing the structure that is represented in Figure 1.7 [47, 48]. FDA has approved gum guar for secure human usage, being normally utilized as a dietary fiber, thickener in lotions and creams, tablet binder, emulsion stabilizer and also as a controlled release polymer, due to its high hydration rate.

Guar gum is constituted by long chains of α-D-mannopyranosyl units linked together by β-D-(1-4)-glycosidic linkage. Side groups of α-D-galactopyranose appear linked to the main mannose chain, in a ratio of mannose to galactose of approximately 2:1. The molecular weight of guar gum is estimated to be around 200.000 to 300.000 daltons [52].

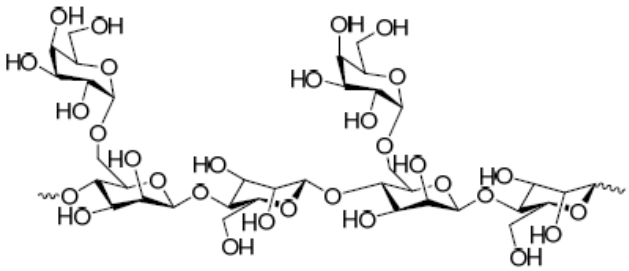

Figure 1.7 – Chemical structure of guar gum.

Due to its high molecular weight and ability to incorporate water, guar gum forms very viscous solutions that impose various limitations in the processing and application of the molecule. There is a commercial variant consisting of partially hydrolyzed guar gum (PHGG), which is produced by partial hydrolysis with β-endo-mannanase or pectinase, which presents lower molecular weight (with an average of 20.000 daltons) and, consequently, viscosity [53]. The whole process of hydrolysis is described on a representative scheme below (Figure 1.8).

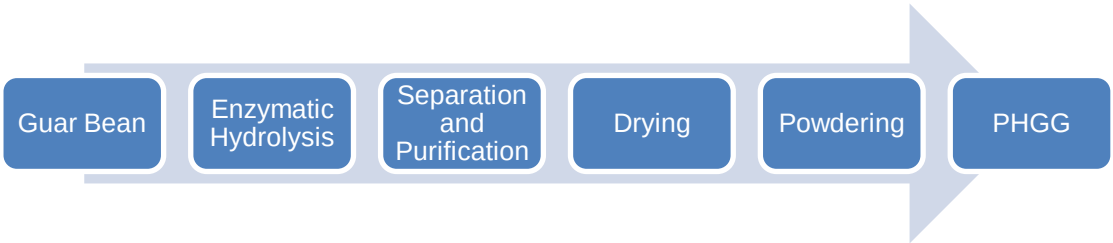

Figure 1.8 – Manufacture scheme of PHGG, step by step.

Adapted from: Yoon *et al*, J Clin Biochem Nutr, 2008 [52].

Microencapsulation might be processed by a variety of physical and chemical methods, including extrusion, spray-drying, coacervation and polymerization, among others. The selection of a method is strongly dependent on the final application of the microparticles and the required

properties of the carriers [50]. Spray-drying is considered a mild technique and is one of the most used, particularly regarding applications in inhalation. It permits the control of microparticle properties (i.e. size, density and shape) depending on the operating conditions. Additionally, it offers rapid processing and is a continuous and one step process, which guarantees simplicity and cost effectiveness. The process consists firstly on the entrance of a drying gas (air, nitrogen) at the top of the spray-dryer apparatus (Figure 1.9), where it is heated to a previously set temperature. The gas interacts with the liquid formulation being simultaneously introduced in the nozzle of the equipment, resulting in the formation of a spray. The high temperature induces the evaporation of the liquid of each formed droplet, thus only remaining the solid content of each of the droplets, which corresponds to the microparticles. These are separated by a cyclonic separator and accumulate in the collecting vessel, from which they are collected at the end of the process, using a rubber and/or metallic spatula [50, 51].

Figure 1.9 – Diagram of spray-drying method. Aqueous solution is fed through Büchi B-290 Mini Spray Dryer, where the solvent is evaporated, and spray-dried powder (microparticles) is collected at the end of the process.

In some cases, spray-dried formulations include excipients such as mannitol (Figure 1.10), lactose or leucine, which are included to modulate the stability, drug release or flowing properties of the resulting powders [50].

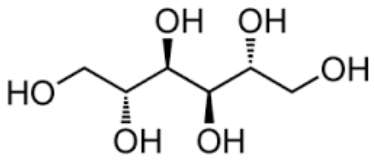

Figure 1.10 – Chemical structure of excipient mannitol.

Chapter II – Aims

2.1. Main aim

- ✓ To evaluate PHGG microparticles as carriers of antitubercular drugs for delivery via inhalation.

2.2. Partial aims

- ✓ To evaluate the crystallinity pattern of PHGG microparticles containing antitubercular drugs;
- ✓ To determine drug association efficiency and drug release profiles;
- ✓ To evaluate the cytotoxic behaviour of drug-loaded PHGG microparticles in relevant cell lines (A549, Calu-3 and differentiated THP-1 cells) for the objective of pulmonary delivery in the ambit of tuberculosis therapy;
- ✓ To determine the minimum inhibitory concentrations of drug-loaded microparticles in relevant bacterial strains for the aim of tuberculosis therapy (*M. bovis and M. smegmatis*);
- ✓ To determine *in vitro* the therapeutic effect provided by drug-loaded PHGG microparticles.

Chapter III - Materials and Methods

3.1. Microparticle preparation

Microparticles based on partially hydrolyzed guar gum (PHGG, Taiyo Kagaku, Japan) were prepared from solutions of the polymer at a concentration of 2% (w/v). A formulation of PHGG microparticles containing mannitol (Man, Sigma-Aldrich, Germany) was also prepared. In that case, a solution of PHGG at 2% (w/v) was prepared and mannitol dissolved directly in this solution to a final concentration of 0.5% (w/v).

Isoniazid (INH, Sigma-Aldrich, Germany) and rifabutin (RFB, Chemos GmbH, Germany) were the antitubercular drugs associated to the microparticles, either individually or in association. Microparticles containing INH were prepared using a matrix of PHGG:Man (PHGG at 2% and mannitol at 0.5% as described before). All other formulations, either containing rifabutin or the association of both drugs, were prepared in a matrix of PHGG only. In summary, 5 formulations were prepared, with the denominations described as follows (in parenthesis is indicated the mass ratio between materials): PHGG; PHGG:Man (10:2.5); PHGG:Man:INH (10:2.5:1); PHGG:RFB (10:1); PHGG:INH:RFB (10:1:1). In all cases, the final volume of the aqueous solution prepared for spray-drying was 30 mL. Both drugs required grinding in a mortar prior to solubilization in Milli-Q water. In the case of RFB, it was further needed to add HCl to obtain a clear solution. Briefly, in the case of INH-loaded microparticles (no RFB present), PHGG was solubilized in water at a concentration of 2% (w/v). Mannitol was then solubilized directly into this solution to a final concentration of 0.5 % (w/v). In parallel, INH was grinded in a porcelain mortar and then solubilized in water. The obtained INH solution was then added to the previous solution of PHGG:Man, and left under stiriring (Velp Scientifics, Italy) for 20 minutes. INH was added to have a final concentration of 10% with respect to the polymer, thus representing a polymer/drug ratio of 10:1 (w/w). For RFB-loaded microparticles, PHGG 2% (w/v) and RFB were simultaneously grinded in a glass mortar and then solubilized in Milli-Q water. In order to achieve an optimum dispersion in the presence of an hydrophobic drug such as RFB, the addition of HCl (Sigma-Aldrich, Germany) proved to be useful, as it protonates the drug. HCl was used at the concentration of 0.001 M and a satisfactory dispersion was obtained with 1.4 mL. The resulting solution was left under stirring for 40 minutes. RFB was added to obtain a final concentration of 10% with respect to the polymer, also representing a polymer/drug ratio of 10:1 (w/w). Finally, in the case of the formulation containing both drugs, PHGG 2% (w/v) and RFB were grinded simultaneously in a glass mortar, whereas the same amount of HCl 0.001 M was added. Another solution, with INH, was prepared separately as described above. Both solutions were mixed under stirring for 40 minutes. The final polymer/drug ratio for PHGG:INH:RFB microparticles was 10:1:1 (w/w).

Dry powder formulations were obtained by spray-drying (Büchi B-290 Mini Spray Dryer, Büchi Labortechnik AG, Switzerland), with the equipment operating in an open mode configuration,

with compressed air used for the evaporation of the solvent of the aqueous solution. The parameters for the spray-drying of PHGG to obtain the MPs with the desired characteristics for deep lung delivery were previously optimized by Ana Grenha's team and are shown in Table 3.1.

Table 3.1 – Spray-drying parameters for the production of PHGG-based microparticles (air flow set at 400 Nl/h).

Formulation	T inlet (º C)	Aspirator (%)	Feed speed (mL/min)	T outlet (º C)
PHGG	160 ± 1	80	1	90 ± 4
PHGG:Man	170 ± 1	80	2	98 ± 2
PHGG:Man:INH	175 ± 1	85	1	104 ± 3
PHGG:RFB	160 ± 1	80	1.5	91 ± 4
PHGG:INH:RFB	170 ± 1	75	1.5	96 ± 3

The production of each formulation was repeated in triplicate (n = 3). All dry powders were stored in desiccators until further use. The aqueous solutions and the resulting dry powders loaded with drugs were protected from light in every step of manipulation and storage.

3.2. Microparticle characterization

Microparticle surface morphology was characterized by field emission scanning electron microscopy (FESEM, Ultra Plus, Zeiss, Germany). Production yield of the process was calculated based on the comparison of total solids weight with the resultant powder weight after spray drying, through the following equation:

$$\text{Production Yield } (\%) = \frac{\text{Microparticles weight}}{\text{Total solids weight}} \times 100 \quad \text{(Eq.1)}$$

Size was assessed manually by optical microscopy (Microscope TR 500, VWR International, Belgium) as the Feret's diameter (estimation of 300 microparticle measurement for each replicate). Tap density was obtained by measuring the volume of a known weight of powder upon being placed in a 10 mL graduated cylinder after mechanical tapping (30 tap/min) using a tap density tester (Densitap, Deyman, Spain). After registration of the initial volume, the tapping process continued until constant volume was achieved according to the method description made in [44]. Bulk density was determined as the ratio of the mass to the volume of the powder samples after inserting the powder in a graduated cylinder. Real density was determined using a Helium pycnometer (Accupyc II 1340, Micrometrics, USA). A theoretical estimation of the

aerodynamic diameter was calculated using the values of real density and Feret's diameter, through the following formula:

$$d_{ae} = d_g \times \sqrt{\frac{\rho_{real}}{\chi}}$$

(Eq.2)

Where d_{ae} represents aerodynamic diameter; d_g is the geometric diameter (Feret's diameter), ρ_{real} is the real density and χ represents the shape factor of MP (1 for spherical microparticles; 2 for irregular microparticles). Carr's Index is a parameter that measures the microparticles flowability. It derives from bulk density and tapped density data and values lower than 25% indicate an optimum flowing pattern, between 20-30% still indicates good powder flow properties [56, 57]. The Carr's index was calculated based on the following formula:

$$\text{Carr's index } (\%) = \frac{\text{Tap density} - \text{Bulk density}}{\text{Tap density}} \times 100$$

(Eq.3)

3.3. Determination of powder cristallinity

The crystalline pattern of the original polymer (PHGG), pure drugs INH and RFB, and spray-dried microspheres was assessed by Powder X-ray diffraction. All the produced microparticle formulations, as referred in section 3.1., were analyzed. A representative replicate of each formulation was analyzed with a PANalytical X'Pert Pro diffractometer using CuKα radiation filtered by Ni and an X'Celerator detector. The patterns were obtained by reflection mode from 5º to 70º 2θ, at a step rate of 0.05º and 1500 seconds per step, with the diffractometer operating at 45 kV and 35 mA.

3.4. Drug association efficiency and loading capacity

In order to determine the amount of drug associated to each formulation, the samples were dissolved using different protocols. PHGG:RFB microparticles (20 mg) were dissolved in 10 mL of HCl 0.1M; PHGG:INH:RFB microparticles (10 mg) were dissolved in 20 mL of HCl 0.1M and 5 mg of PHGG:Man:INH were solubilized in 20 mL of 0.1M HCl. After dissolution, the solutions were filtered (0.45 µm) and retained for further analysis. The drug content was determined by spectrophotometry (UV-1700 Pharmaspec, Shimadzu, Japan) at 268.5 nm (INH) and 500 nm (RFB), after establishing calibration curves. The association efficiency (AE) was calculated as the ratio between the real amount of drug contained in the MPs and the theoretical quantity added to prepare the microparticles. The calculation was made using the following equation:

$$\text{AE}\ (\%) = \frac{\text{Real amount of drug in MP}}{\text{Theoretical amount of drug added for MP formulation}}\ \text{x}\ 100$$

(Eq. 4)

The drug loading capacity (LC) was calculated as the recovered drug mass (real amount) as a function of MPs weight:

$$\text{LC}\ (\%) = \frac{\text{Real amount of drug on MP}}{\text{Weight of MP}}$$

(Eq. 5)

3.5. *In vitro* drug release profile

The drug release profile of each formulation was determined in a medium representative of the lung lining fluid. This medium is composed of Phosphate Buffered Saline (PBS, VWR, USA) pH 7.4, thus representing the local pH of the lung, added of 1% (v/v) Tween® 80 (Merck, USA), which represents the lung surfactant. The assays were conducted respecting sink conditions. An amount of 15 mg of PHGG:RFB and PHGG:INH:RFB microparticles were incubated in 10 mL of release medium and placed under stirring (100 rpm) at 37 ºC. At pre-established time intervals from 5 to 90 minutes, samples were collected, filtered (0.45 µm) and drugs quantified by UV-Vis, as described above. Adequate calibration curves were established. The assays were performed in triplicate.

3.6. Cell Lines

Cell lines representative of the lung epithelia were used. A549 cells (American Type Culture Collection – ATCC CCL-185, USA), representative of alveolar epithelium, were used between passages 35-45; and Calu-3 cells (ATCC HTB-55, USA), representative of bronchial epithelia were used between passages 20-31. THP-1 cells (DSMZ, ACC 16, Germany), a human monocytic cell line, were used between passages 12-22. Both A549 and Calu-3 cells were cultured in DMEM (Sigma-Aldrich, Germany), supplemented with 10% (v/v) Fetal bovine serum (FBS, Gibco, USA), 1% (v/v) non-essential aminoacids (Gibco, UK), 1% (v/v) L-glutamine 200 mM (Gibco, UK) and 1% (v/v) penicillin/streptomycin (VWR, Germany). THP-1 cell line was cultured in RPMI 1640 medium (VWR, Belgium), supplemented with 10% (v/v) FBS, 1% (v/v) L-glutamine 200mM and 1% (v/v) penicillin/streptomycin.

All the cultures were maintained in 75 cm^2 T-flasks, in an incubator at 37 ºC and 5% CO_2. In all cases the medium was changed each 2-3 days, A549 and THP-1 cells were subcultured every week, while, Calu-3 cells were submitted to the process each 15 days. A549 and Calu-3 cells are adherent cells and required the use of trypsin/ EDTA (Sigma-Aldrich, Germany) for detaching process required for subculturing.

THP-1 cells remain in suspension, and were into macrophage-like cells upon a specific treatment. This consisted in adding 50 nM phorbol myristate acetate (PMA, Sigma-Aldrich, Germany) into the medium during 48 hours, followed by a period of 24 hours incubation in cell culture medium without PMA.

3.7. Evaluation of microparticle cytotoxicity

The cytotoxicity of microparticles was assessed on the cell lines mentioned above. The cytotoxic profile was evaluated using two different techniques, the 3-(4,5-dimethylthiazol-2-yl)-2,5-diphenyltetrazolium bromide (MTT, VWR, USA) assay and the determination of released lactate dehydrogenase (LDH). The MTT assay is based on the formation of formazan by the reduction of the tetrazolium salts by mitochondrial reductases present on metabolic active cells dependent of NAD(P)H, as is shown in Figure 3.1. The amount of formed formazan reflects the number of viable cells. Therefore, low cell viability results on a minor spectrophotometric signal.

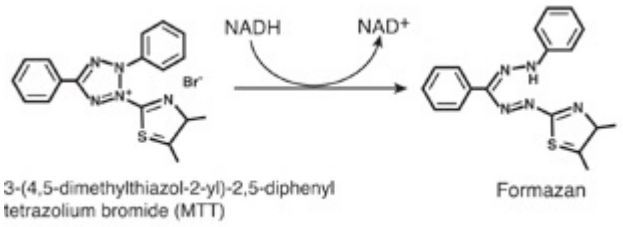

Figure 3.1 – Basic principle of the MTT assay. Yellow tetrazolium salt is reduced by mitochondrial reductases into dark red/purple formazan.

Adapted from: Liu and Nair, J. Nat. Prod., 2010 [58].

All developed formulations were tested at the concentrations of 0.1, 0.5 and 1 mg/mL. Cell culture medium (CM) and dodecyl sodium sulphate (SDS, Sigma-Aldrich, Germany) at a concentration of 2% (w/v) were tested as positive and negative controls of cell viability, respectively. Therefore, the result of CM represents 100% of cell viability. Cells at an appropriate density of 0.1 or 0.2 x 10^{6} for A549 and Calu-3 cells, respectively, were cultured in 96 well plates and allowed to adhere for 24 hours. After that time, the medium was removed and replaced for a DMEM medium without FBS containing the samples (microparticles formulations and antitubercular drugs microparticles). Removing the FBS avoids any interference of proteins with the solutions and controls. The formulations and controls to be tested were incubated with the cells during 3 or 24 hours. After that procedure, MTT (0.5 mg/mL in PBS, pH 7.4) was added for an incubation of 2 hours. The formed formazan crystals were solubilized with dimethyl sulphoxide (DMSO, VWR Chemicals, France) and the absorbance was measured by spectrophotometry (Infinite M200, Tecan, Austria) at 540 nm (background correction at 650 nm). For THP-1, the reagent used for the solubilization of formazan crystals was SDS 10% and a short period of stirring (30 minutes, 150 rpm, 37 ºC) was required to

promote a better dissolution. In that case, 96-well plates were read at 570 nm (background correction at 650 nm).

The following formula was used to determine the cell viability:

$$Cell\ viability(\%) = \frac{(\mathrm{Abs} - \mathrm{S})}{(\mathrm{CM} - \mathrm{S})}$$

(Eq.6)

Where Abs stands for absorbance of the test substance, CM is the absorbance upon incubation with culture medium, and S the absorbance for negative control SDS 2%.

The LDH assay is a procedure to measure either the number of cells via total cytoplasmatic LDH or membrane integrity as a function of the amount of cytoplasmic LDH released into the medium. LDH catalyzes the conversion of lactate to pyruvate, based on the reduction of NAD^+ to NADH. Then diaphorase uses NADH to reduce iodonitrotetrazolium (INT) to a red formazan product (Figure 3.2). The resulting colored compound is measured spectrophotometrically. The greater the loss of integrity, the greater will be the read absorbance (reflecting higher amount of released LDH).

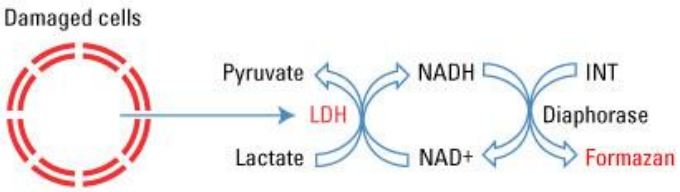

Figure 3.2 – Basic metabolic reaction occuring in LDH assay.

Reprinted from: www.lifetechnologies.com

The formulations were generally tested at the concentration of 1mg/mL, although those containing rifabutin as sole drug and incorporated in formulations, were also tested at the concentration of 0.5 mg/mL. The same set of experiments used for the MTT assay (which directly used the cells for the assay procedure) was used for the LDH assay, in this case analyzing the supernatant of cells upon incubation with samples. A specific kit was used to perform the assay (LDH kit, Sigma-Aldrich, USA). CM and a lysis buffer provided in the kit were tested for the released LDH as controls, and a non-cytotoxic effect is described for a value until 100%. The value obtained for CM is considered 100% LDH and assumed as regular/normal LDH release.

Aliquots (100 μL) of cell supernatant samples were removed from the cell plates upon exposure to the formulations/drugs. The aliquots were placed into eppendorfs and centrifuged at 16.000 x g for 5 minutes. The supernatant obtained upon centrifugation was transferred (50 μL) to a new 96-well plate and 100 μL of the tampon mix (substrate solution, preparation cofactor and dye

solution from the LDH kit) were added. After 20 minutes, the reaction was stopped with 15 µL of HCl 1.0M. The absorbance was measured by UV/Vis spectrophotometry, at 490 nm (background correction at 690 nm).

The % of released LDH was determined based on the formula:

$$\text{Released LDH } (\%) = \frac{\text{Abs}}{\text{CM}} \text{ x}100$$

(Eq. 7)

Where Abs stands for absorbance corresponding to incubation with test samples and CM is that resulting from the incubation with culture medium.

3.8. Bacterial strains and growth conditions

The mycobacterial strains used were the *M. smegmatis* 4XR2 that was a gift from Professor Peter Andrew, Department of Infection, Immunity and Inflammation, at Leicester, UK; and the *M. bovis* BCG DSMZ 43990. Both strains were cultivated in Middlebrook 7H9 (M7H9) broth (Remel, Lenexa, USA) (users recommendation of 4.7 g per liter), supplemented with 10% OADC (oleic acid, albumin, dextrose and catalase) (Remel, Lenexa,USA). The addition of 0.5% (w/v) of aqueous kanamycin (0.005 mg/mL) (Fisher Scientific, China) and 0.2% (v/v) of glycerol (Sigma-Aldrich, Germany) was used for *M. smegmatis* growth. In fact, *M. bovis* does not degrade carbon sources like glycerol, so the medium for *M. bovis* was devoid of it [1]. The addition of 0.05 % of Tween® 80, allowed a better observation of growth of this strain.

Mycobacteria were manipulated observing safety rules, inside a laminar flux chamber (Bio48 Faster, Italy) to prevent infection. All the material in contact with the bacteria was sterilized by autoclave (Uniclave88, Portugal). The stocks of bacteria were conserved and stored inside an ultra-low temperature freezer -80 ºC (U725 Innova New Brunswick Scientific, USA).

M. smegmatis 4XR2 was grown at 37 ºC for 2 days in liquid medium (M7H9), then transferred to solid medium, M7H9 prepared with bacteriological agar type E (Biokar diagnostics, France) to ensure the purity of the colonies for 3 days. Then, it was again transferred to liquid medium to proceed with growth assays. The assays were conducted after achieving an optical density value (OD_{nm}) of approximately 0.2., at 600 nm. The bacterial strain *M. bovis* was grown for 21 days. The assays were conducted after the OD reached approximately 0.2. At this point, a live/dead staining was conducted to check the viability of bacteria using the epifluorescence microscope (Axio Imager Z2 Fluorescence microscope, Germany). Nucleic acid stains provide a quick approach to distinguish live bacteria with intact membranes, stained in green (Syto 9), from dead bacteria with compromised membranes, stained in red (Propidium iodide).

3.9. Minimal inhibitory concentration (MIC) determination

MIC is defined as the concentration of antimicrobial agent, such as an antibiotic, required to inhibit the bacterial growth [59]. Determination of antibiotic MIC plays an important role to measure their susceptibility to the drug. The MTT assay was adopted to quantify bacterial cell viability, as it is easily detected through colour change [60]. The INH (Sigma-Aldrich, Germany) stock solution was prepared at a concentration of 1 mg/mL in a solution of PBS. The RFB (Chemos GmbH, Germany) stock solution was prepared at the concentration of 1 mg/mL in a solution of DMSO. To guarantee sterility, the solutions were filtered with a disposable 0.22 µm sterile filter. When in association, a mixture of the antibiotics was dissolved in a 50:50 PBS:DMSO solution. Based on the calculations to achieve the desired concentrations, the stock solutions were then diluted in complete medium (M7H9). A solution of the higher drug(s) concentration was prepared in complete medium and 360 µL introduced directly in the designated wells of 96-well flat-bottom microplates (Orange Scientific, Belgium). Two-fold serial dilutions were continuously made using a multichannel pipette.

INH concentrations varied between 32 and 0.5 µg/mL, while RFB concentrations were from 0.8 to 0.025 µg/mL. *M. smegmatis* was initially cultured in 7 mL of fresh M7H9 complete medium, in triplicate, and adjusted to a McFarland 1.0. Then, the bacteria were centrifuged and transferred to 1 mL eppendorfs containing the ressuspended inoculums in complete medium, M7H9. A 20 µL of this bacterial suspension was introduced into the wells containing 180 µL of drug dilutions (completing the final volume of 200 µL per well). Each bacterial triplicate (1, 2 and 3) was added in A-B, C-D, and E-F rows, respectively. The bottom lines (H-G) were dilution controls, no bacteria was inoculated. Columns 2 and 4 represent negative (culture medium, 200 µL) and positive control (bacteria 20 µL + 180 complete medium with no agent), respectively, as shown in Figure 3.3.

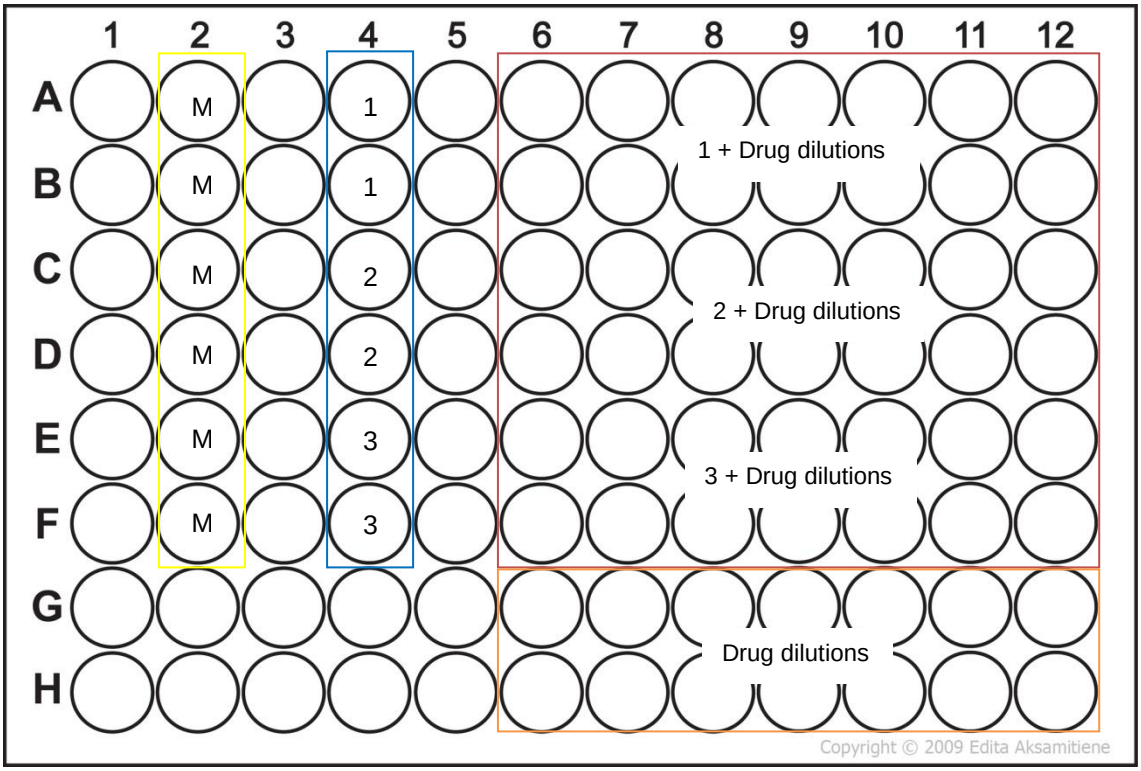

Figure 3.3 –The 96-well plate template in which column 2 had the medium (M) and column 4 the bacteria in triplicate, 1, 2 and 3 respectively. The columns 3-12 and rows A-F, contained the various drug dilutions with bacteria, and the rows G-H the drug dilutions in absence of the bacteria. The assay was done using 6 technical replicates (n=6).

The plates were covered, sealed with parafilm and incubated at 37 °C (Binder, USA). After 18 hours of incubation, 30 µL of MTT sterile solution were added to each well. A 6 hour period of incubation was allowed (completing 24 hours), after which 50 µL of DMSO were introduced into wells, resulting in a change of colour from yellow to dark gold for growing bacterial cells. Data was retrieved from the plate reader at 540 nm. Agar plates with solid media M7H9 were also used, in order to examine the recovery of viability. For this drops of 10 µL from the 96 well plates were transferred to the agar plates (before adding MTT). MICs were obtained based on these two methods. To test the MIC corresponding to MPs, the powders of each formulation were weighed into a test tube and sterilized by UV light, for 15 minutes. Then the samples were solubilised and the higher concentration was prepared in complete liquid medium M7H9 and added to the 96-well plates, based on the same protocol made for drug solutions. The established concentrations were on a range of 32 to 0.5 µg/mL (MPs with only INH), 0.8 to 0.025 µg/mL (MPs with only RFB), and 2 to 0.125 µg/mL (MPs with the association of drugs).

The same process was carried out for *M. bovis*, but the outside lane (a frame-like) was all filled with fresh medium (or sterile water), thus avoiding the evaporation of liquid from the wells. The inside wells were used to proceed with the MIC determination. The established higher concentrations of individual drugs, drug association and MPs were established at 1 µg/mL and

diluted two-fold. After 7 days of incubation, MTT was added and 24 hours of incubation were allowed before adding DMSO in order to retrieve a reliable result.

3.10. Infection procedure

THP-1 human derived macrophage-like cells were cultivated in RPMI 1640 complete medium and incubated at 37 ºC in 5% of CO_2, starting with a cellular density of $0.2x10^6$ cells/mL [60]. THP-1 cells were differentiated into macrophages with a treatment of 48 hours with 50 nM of PMA and left for an additional 24 hours in absence of PMA allowing the cell line to recover [61]. The resulting adherent host cells were counted for the 24 well plates (Orange Scientifics), where a procedure of 4 and 24 hours of infection took place. The cell medium was replaced with the bacterial growth medium.

In the case of *M. smegmatis* that forms clumps, a brief sonication of 5-10 minutes disaggregates them. An OD of 0.1 at 600 nm from the suspension corresponds to 1 x 10^7 bacteria per mL [62]. Based on this fact an estimated a multiplicity of infection (MOI) of 10 was achieved, obtaining the desired volume of bacteria to add into each well (approximately 100 µL in each well) [61, 62]. The cells were left in contact with the bacteria for 3 hours inside an appropriate incubator (Sanyo CO_2 incubator MCO-18AIC, Japan) [56, 57]. The culture medium was removed and the infected cells were washed three times with sterile PBS 1x, in order to remove the bacteria that were not captured by macrophages. The antibiotics and MPs were dissolved in bacterial medium at the MIC value previously determined for the formulation with both drugs. The solutions were added into the defined wells. The associated drugs and loaded MPs with INH and RFB were in contact with the infected macrophages, for 4 and 24 hours. The 24-well plates were divided into three groups, as presented in Figure 3.4.

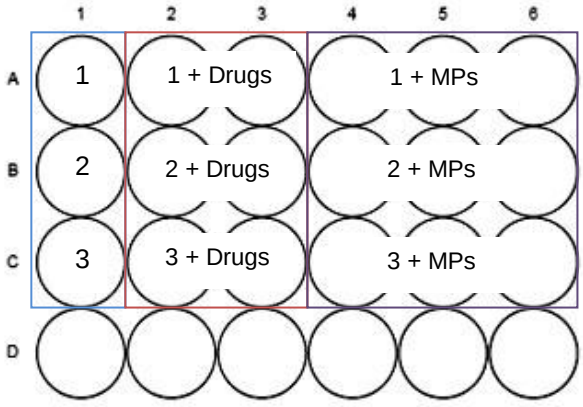

Figure 3.4 – Scheme of the 24-well plate. Column 1: infected cells with *M. smegmatis* triplicates (1, 2 and 3); Columns 2 and 3: infected cells with associated drugs (INH and RFB), MIC =1 µg/mL. Columns 4, 5 and 6: infected cells with MPs loaded with both drugs, same MIC.

The lysis agent Triton X-100 (Ameresco, USA) was added (1 mL, 1:100) to each well after washing with PBS again, in order to lyse the cells but not the bacteria. The plate rested during 15 minutes, at room temperature. The suspension was mixed several times using an automatic pipette, 20 µL were taken from the suspension and added to 180 µL M7H9 on 96-well plates. Serial dilutions were made, passing 20 µL of the content. The dilutions ranged 10^{-1} – 10^{-6}.

Drops of 10 µL were inoculated into agar plates and incubated at 37 ºC in a CO_2 incubator to allow the mycobacteria growth under these conditions, in order to observe the free drug effect and MPs effect against the mycobacteria. MTT procedure was performed on the 96-well plates, as described above, to determine bacterial viability. For counting the bacterial cells 10 µL of each dilution were inoculated into agar plates and incubated at 37 ºC. After 24-48 hours the colonies became visible and were counted with the help of a magnifier [62].

3.11. Statistical analysis

The *t*-test and the one-way analysis of variance (ANOVA) with the pairwise multiple comparison procedures (Student–Newman–Keuls method) were performed to compare two or multiple groups, respectively. The analysis was made using the SigmaStat statistical program (Version 1, Jandel Scientific, USA) and differences were considered to be significant at a level of $p < 0.05$.

Chapter IV – Results and Discussion

4.1. Microparticle preparation and characterization

As stated in the methodology, several formulations of microparticles based on PHGG were produced aiming at an application as inhalable treatment of lung tuberculosis. The literature only refers the use of guar gum in pharma applications regarding the formulation of oral systems [50–52]. However, the majority of gum guar related works are devised to food applications. In this work, two model antitubercular drugs were associated (INH and RFB) with microparticles, which were produced with the required characteristics to enable inhalation. In this regard, considering that MTB is hosted by alveolar macrophages, the designed microparticles need to reach the alveolar zone, which requires good flowing properties.

The formulation comprising only PHGG was the only one not enabling adequate optimization, as the formation of large agglomerates could not be prevented by the combined modification of the parameters of the spray-dryer. In that case, poor flowing properties were macroscopically observed for the resultant dry powder, which was in line with the calculated Carr's index, displayed in Table 4.1 (32 ± 6%). All other formulations had been previously optimized by Ana Grenha's team, and were reproduced with success during this work. It was verified macroscopically that the presence of RFB improved the flowability of the dry powders (the Carr's index of PHGG:RFB microparticles was the lowest, 26 ± 7%, while that of PHGG:INH:RFB microparticles was 31 ± 4%). Therefore, formulations containing this antibiotic could be developed comprising PHGG by itself as matrix material. On the contrary, as INH was not observed to induce the same effect on flowability, the formulation containing only INH (PHGG:Man:INH) had to be added of mannitol to achieve the desired flowing properties. Although the flowing ability of this formulation was satisfactory macroscopically, the relatively high Carr's index value was 30 ± 5%. The inclusion of mannitol in order to improve flowing properties was previously reported in the literature and was also demonstrated in previous works of the group [50]. It is important to mention that, in spite of the obtained Carr's index values above the recommended 25%, the flowability of the optimized microparticle formulations was considered reasonably good [56].

Microparticle morphology was verified by FESEM and the respective microphotographs are depicted in Figure 4.1.

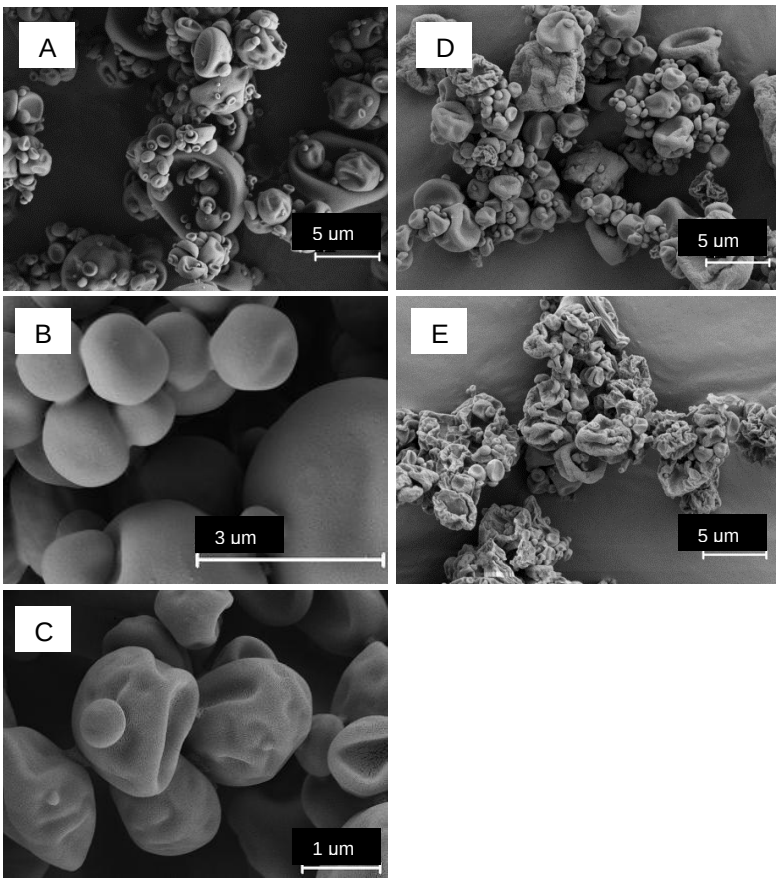

Figure 4.1 – FESEM microphotographs of different formulations of microparticles. A) PHGG, B) PHGG:Man, C) PHGG:Man:INH, D) PHGG:RFB, E) PHGG:INH:RFB.

In this figure, two kinds of morphology are perceptible. PHGG:Man MPs, displays a more spherical and smooth surface, while all the other formulations show various surface irregularities. PHGG MPs show a convoluted and irregular shape, which becomes more spherical when mannitol is added. This phenomenon is reported in other works where mannitol also produces spherical particles [65]. The surface of microparticles obtained by spray-drying pure INH has been reported to usually show corrugations [11]. However, PHGG MPs combining both INH and mannitol produced in this work, the surface has only a slight corrugated effect and the particles are almost spherical. Pure RFB also shows an irregular shape upon spray-drying, with rough surface [66]. The interaction of RFB with PHGG matrix in spray-drying was still resulting in microparticles with corrugated surface, as shown in this work. PHGG:INH:RFB microparticles show an even more corrugated morphology. This was expected based on the reports of irregular morphology for both antitubercular drugs upon spray-drying and because, in this formulation, mannitol is not present and it was seen to be the excipient improving the regularity of microparticles. Microparticles with a different matrix composition (polylactic acid), curiously described the same irregular surface when in presence of both associated drugs [31]. A corrugated morphology associated with low tap density (0.1 g/cm^3) is reported to positively

affect powder dispersibility by minimizing the contact areas, and also to lower the aerodynamic diameter, which is essential for an efficient pulmonary drug delivery [45].

The yield of the spray-drying process was calculated at the end of each process, reaching values considered very reasonable and in certain cases inclusive very good (68% - 85%). In fact, it is not very frequent to see in the literature such yield values, which is very relevant, because it means a low loss of materials and indicates the effectiveness of the technique. One of the reasons most likely contributing to this yield values was the use of the high performance cyclone, instead of the conventional cyclonic separator. This cyclone was already reported to improve the production yields [67].

Given the application in inhalation, the prepared formulations were characterized by their aerodynamic properties, which include the determination of the Feret's diameter, tap and real densities, and aerodynamic diameter. The obtained results are shown in Table 4.1.

Table 4.1 – Aerodynamic characteristics of dry powders (Feret's diameter, bulk, tap and real densities, theoretical aerodynamic diameter and Carr's index). (Mean ± Standard deviation, n = 3).

Formulations	Feret's diameter (μm)	Bulk density (g/cm^3)	Tap density (g/cm^3)	Real density (g/cm^3)	Aerodynamic diameter (μm)	Carr's Index (%)
PHGG	1.60 ± 0.77	0.33 ± 0.04	0.50 ± 0.04	1.56 ± 0.08	1.41 ± 0.17*	32 ± 6
PHGG:Man	1.80 ± 0.99	0.32 ± 0.04	0.48 ± 0.02	1.54 ± 0.01	2.23 ± 0.04#	29 ± 7
PHGG:Man:INH	1.54 ± 0.82	0.32 ± 0.06	0.43 ± 0.06	1.52 ± 0.03	1.34 ± 0.03*	30 ± 5
PHGG:RFB	1.63 ± 0.82	0.26 ± 0.04	0.39 ± 0.01	1.51 ± 0.07	1.43 ± 0.05*	26 ± 7
PHGG:INH:RFB	1.75 ± 0.87	0.26 ± 0.01	0.37 ± 0.05	1.51 ± 0.06	1.52 ± 0.02*	31 ± 4

#Shape factor 1 used in calculation; *Shape factor 2 used in calculation.

The characterized properties were not very different among formulations. The Feret's diameter varied between 1.54 and 1.80 μm, while real densities were around 1.5 g/cm^3 in all cases. Similar real density values are frequently reported for spray-dried powders [44]. Regarding the size, a small particle size is reported to confer a higher surface area to volume ratio, which for instance permits higher encapsulation of drugs, but also usually results in rapid release of drugs [68]. Bulk densities were around 0.3 g/cm^3 and tap densities increased a little bit in comparison with the former, which is expected because of the method used for the determinations. Density is the inverse of porosity. Therefore, as bulk density is the measurement of the volume of a known amount of powder that was not submitted to a compression force, many hollow spaces are present and there is an inefficient packing. When the tapping is performed the powder gets compacted, and the hollow spaces are filled with efficacy, thus justifying the increase of tap density when compared with bulk density. The conjugation of real density and Feret's diameter enabled the calculation of the theoretical aerodynamic diameter. For this calculation, the shape

factor was $\chi = 1$ for PHGG:Man microparticles which exhibit a spherical shape, while a shape factor of $\chi = 2$ was considered for the rest of microparticle formulations, having irregular shapes. These factors were assigned according to the shapes observed in FESEM microphotographs and are noted in each case in Table 4.1. The fact that the shape factor assumes different values (1 or 2), which are then applied in the equation referred in section 3.2 to calculate aerodynamic diameter, results in that the microparticles showing a lower aerodynamic diameter are those attributed a shape factor of 2. Aerodynamic diameters varied between 1.3 and 2.2 μm in all cases, suggesting that all microparticle formulations have adequate proprieties for lung delivery, at least from a theoretical point of view. Moreover, considering that reaching the alveolar zone requires aerodynamic diameters between 1 and 3 μm [44, 66], the designed drug-loaded formulations are apparently adequate for the strategy of inhalable tuberculosis therapy. Also important is the fact that macrophage capture is maximized for 1 – 2 μm particles [44], which is absolutely coincident with the characteristics of the developed formulations.

4.2. Microparticle X-ray diffraction evaluation

The diffraction of X-rays consists in the scattering of a beam of X-rays, producing a diffraction pattern. XRD technique is useful to determine whether a compound is stable or unstable, based on a resulting crystalline or a more amorphous structure. A crystalline drug structure has a specific signature for physical and chemical proprieties which influences its solubility, and release profile for example [70].

The diffraction patterns of mannitol (commercially provided) and spray-dried (SD) mannitol are depicted in Figure 4.2.

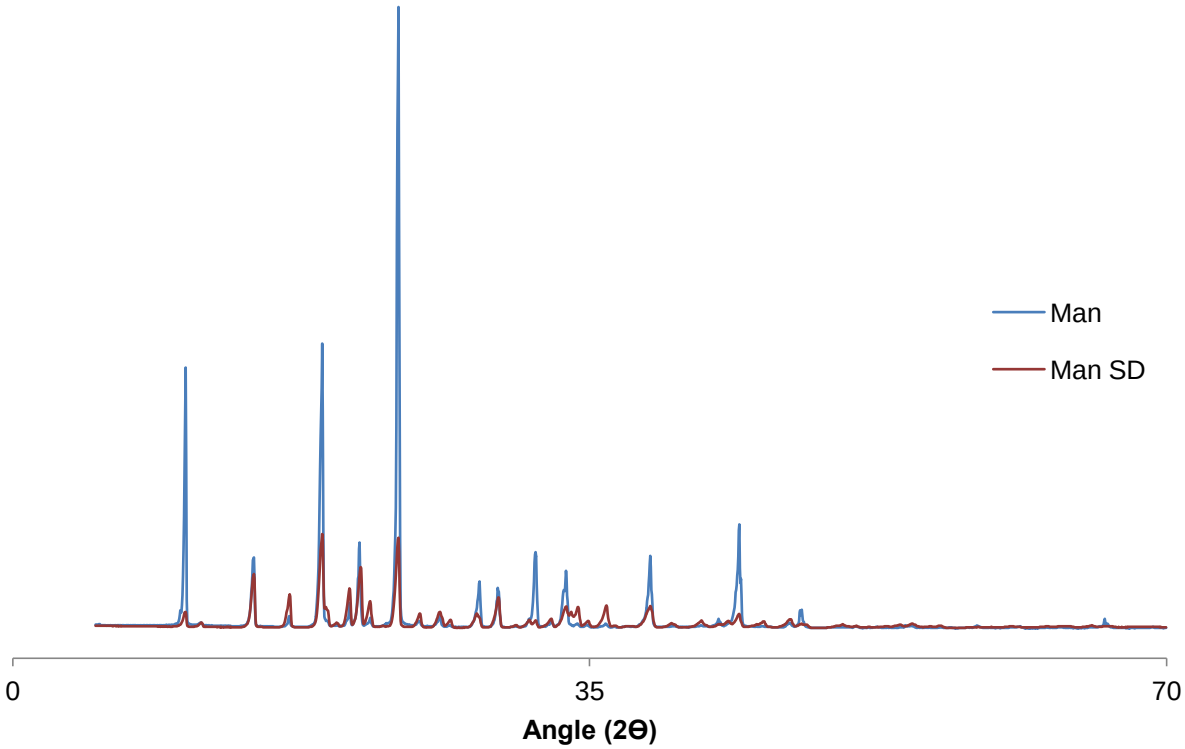

Figure 4.2 – X-ray diffraction patterns of mannitol in pure state and spray-dried (SD) mannitol.

Mannitol (blue) adopts the form of polymorph β [71]. The XRD pattern of mannitol after the spray-drying process (red) shows a significant decrease of the intensity. A very interesting report made by Hulse *et al* (2009) also shows a decrease of mannitol crystallinity [72]. The authors suggest that a difference between intensities of the same substance (for the same amount irradiated) may result from a difference in the size of the crystals or some loss of ordering might be due to the appearance of crystalline defects, residual humidity incorporated in the microparticles or maybe a long storage may also affect the stability. In the case of the present work it is reasonable to accept that the spray-drying process may give rise to smaller crystals of mannitol and broader peaks when compared with the parent material. A plausible explanation for a lower observable intensity relies on rapid crystallization or even dehydration by spray-dying. It should be noted that the same polymorph is observed before and after the spray-drying process [72].

The diffraction patterns of PHGG (commercial) polymer and PHGG spray-dried are represented in Figure 4.3.

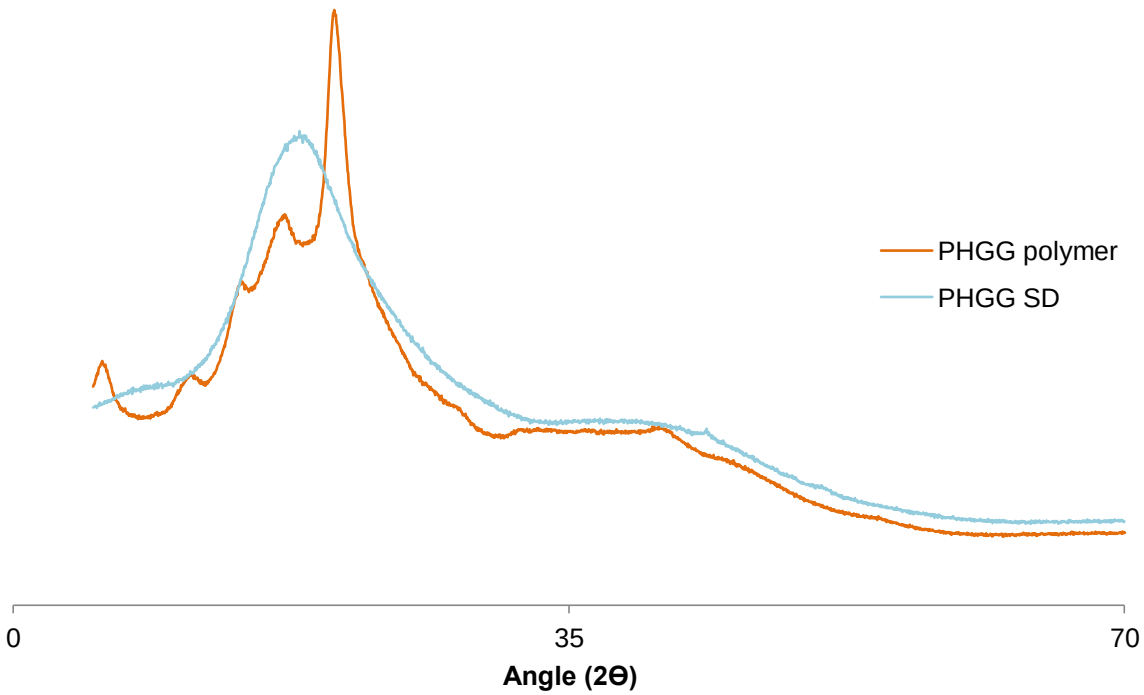

Figure 4.3 – X-ray diffraction patterns of PHGG polymer and spray-dried (SD) PHGG.

The PHGG polymer XRD pattern (orange), displays some broad peaks with low intensity, which indicates some degree of crystallinity. These peaks completely vanish in the pattern of PHGG microparticles (blue). This behavior indicates that the spray-drying process promotes a less ordered arrangement of the polymer chains removing the crystalline domains present in the parent material.

The diffraction patterns of Man SD and PHGG:Man microparticles are represented in Figure 4.4.

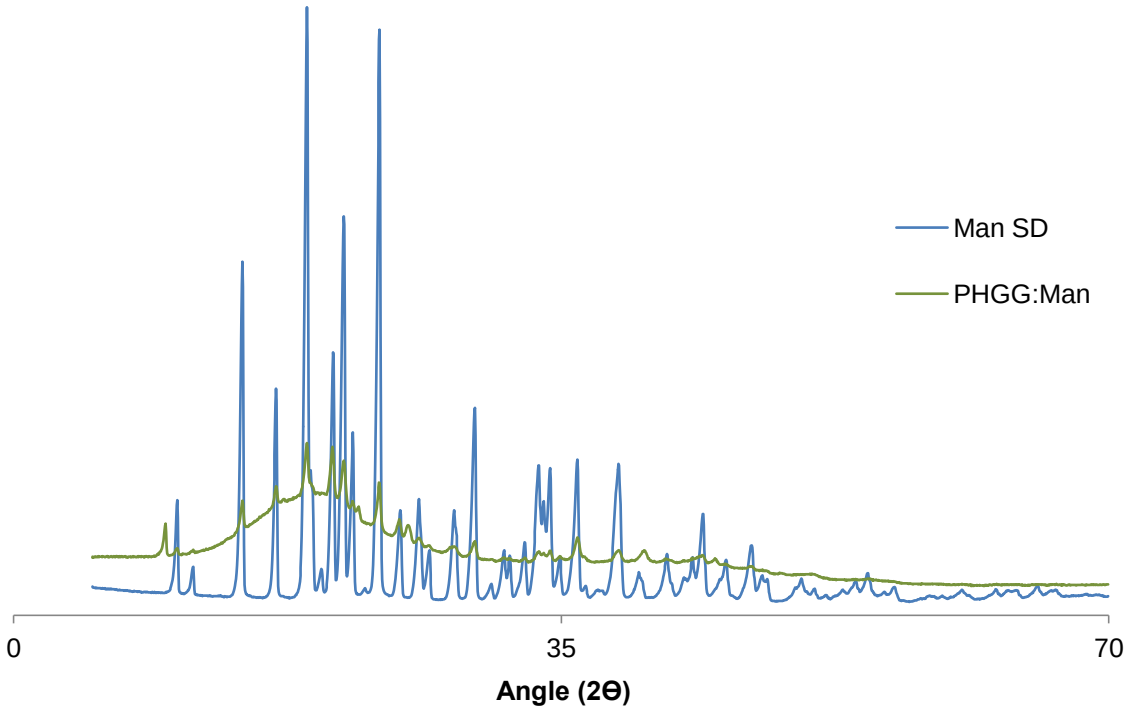

Figure 4.4 – X-ray diffraction patterns of spray-dried (SD) mannitol and PHGG:Man.

The pattern of PHGG:Man (green) exhibits peaks of rather low intensity due to the dilution effect of mannitol onto the polymer matrix. Although the polymorph β could still be identified, the peak at the lowest angle is characteristic of the polymorph γ of mannitol [71]. Comparing the relative intensities of the two polymorphs [65], one can assume that the majority of mannitol present is indeed in the form of polymorph γ. The phenomenon of polymorphism is known as the ability of a compound to crystallize in more than one distinct crystal structure [70]. In this case, different polymorphs will lead to different interaction forces between the polymer and the excipient.

The crystalline structures of each of the formulations containing microparticles related with INH and spray-dried pure INH on its own, were analyzed during XRD, as shown at Figure 4.5.

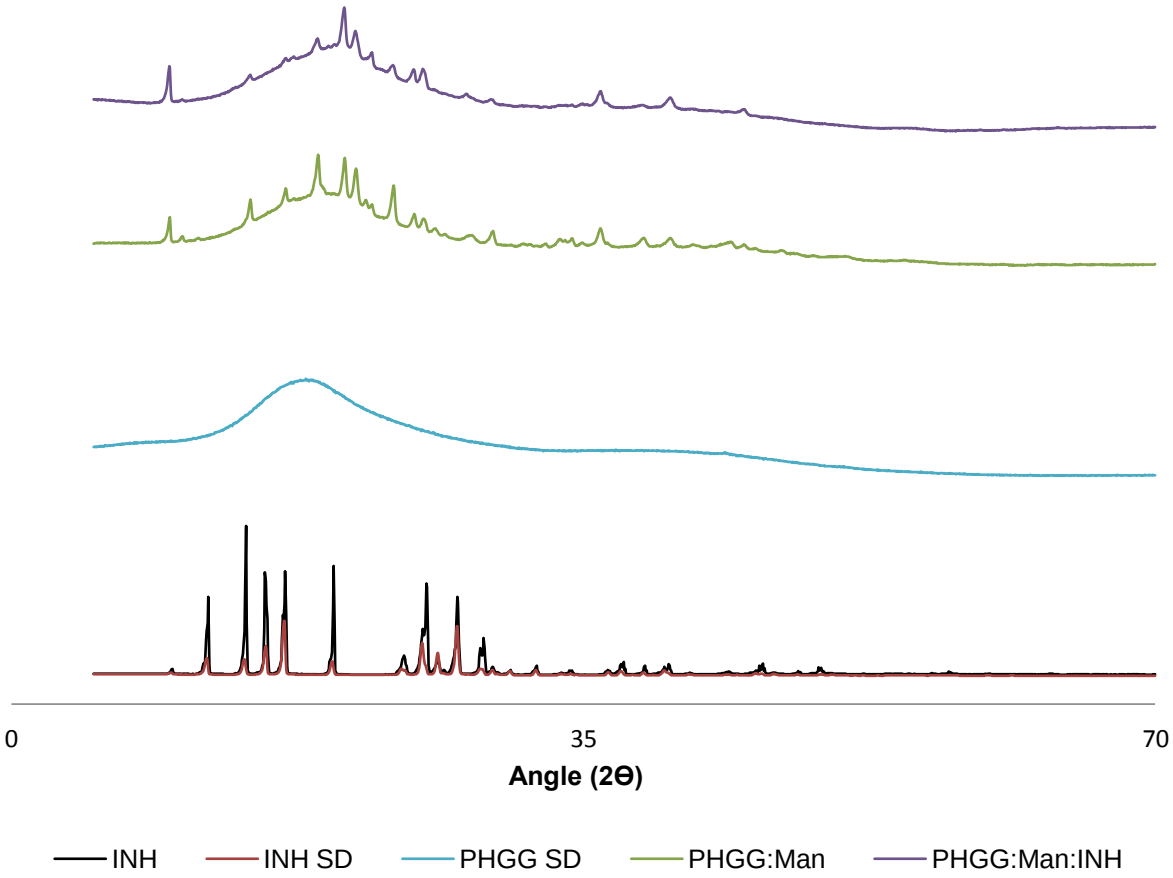

Figure 4.5 – X-ray diffraction patterns of isoniazid (INH) in pure state and spray-dried (SD), PHGG spray-dried (SD), PHGG:Man and PHGG:Man:INH microparticles.

Analyzing the diffraction pattern of INH (black) on its saline form, there is a presence of sharp and intense peaks. After being submitted to spray drying, INH adopts a pattern with less intensity, as observed in the case of mannitol. The same result was reported by Rojanarat *et al* (2011) [65]. PHGG:Man (green) and PHGG:Man:INH (purple) at a 10:1 polymer/drug ratio, exhibit the same baseline of PHGG SD and some characteristic peaks of mannitol polymorphs β and γ, as previously mentioned. The peaks of INH do not transpose into the microparticles, the pattern that prevails is from mannitol polymorphs β and γ. The data obtained for the microparticles do not show the presence crystals of INH in number and/or size to be detected by XRD, which implies that the crystallization process under spray-drying conditions is rather complex and understanding in which ways to maintain its reactional stability requires further experimental efforts.

The crystalline structures of each of the formulations containing microparticles related with RFB and spray-dried pure RFB on its own, were also analyzed during XRD, as shown at Figure 4.6.

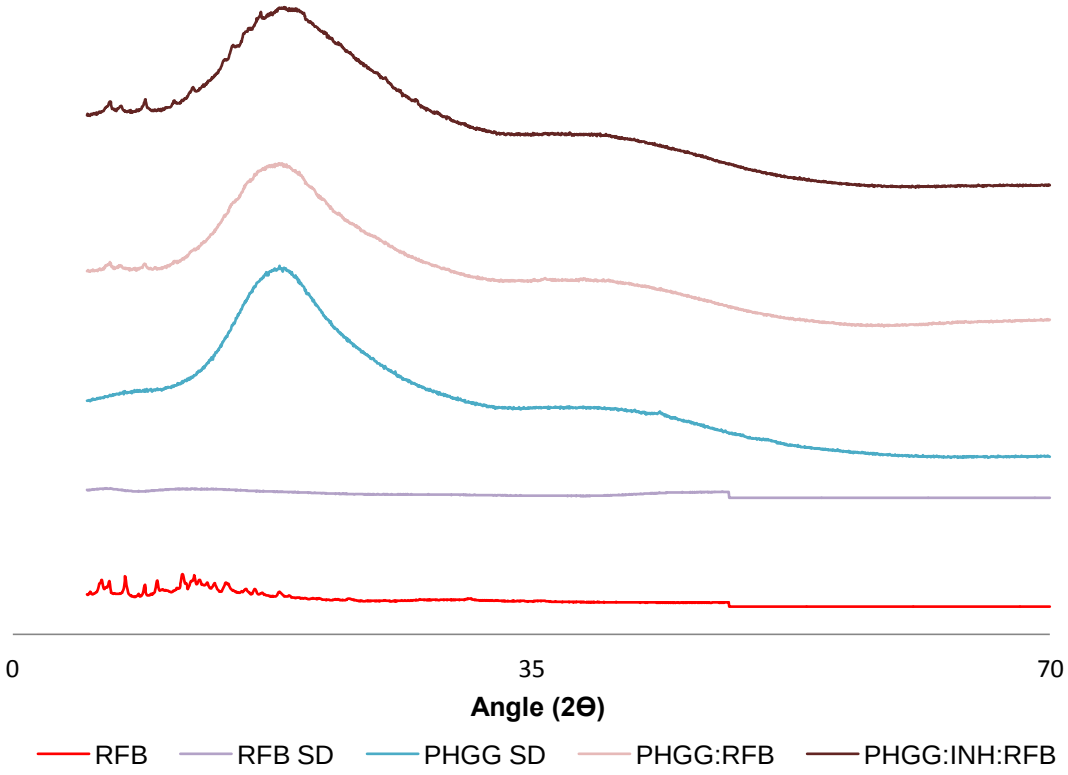

Figure 4.6 – X-ray diffraction patterns of rifabutin (RFB) in pure state and spray-dried (SD), PHGG spray-dried (SD), PHGG:RFB and PHGG:INH:RFB microparticles.

After the spray-drying process, the pattern of RFB does not show any peak of significant intensity. However, the data on the related formulations of PHGG:RFB and PHGG:INH:RFB reveal that, some peaks derived from RFB in pure state, at lowest angles, more conserved. This might be connected to the usage of less concentrated HCl, which did not affect drastically the structure, maintaining some of the drug properties. The results from other data shows a similar profile for RFB drug in pure state [66]. Some compounds could be present in a non-crystalline state, although the existence of small crystals that were not detected by this technique cannot be discarded. The suggestive amorphous pattern displayed at the diffractogram for microparticles loaded with RFB, suggests a possible instability of the compounds, which might be translated in different chemical and physical properties. However, PHGG:INH:RFB seems to maintain a more crystalline form than PHGG:RFB, so comparatively the association of both drugs provides more reactional stability.

4.3. Drug association efficiency and loading capacity

Drug association efficiency and drug loading capacity greatly depend on the solid-state drug solubility in the matrix material, which is related with the polymer composition, the molecular

weight, and the drug-polymer interactions based on the end functional groups [73] (hydroxyl groups in the case of PHGG). Despite important aqueous solubility differences of INH and RFB (125 mg/mL and 0.19 mg/mL, respectively), the association of both drugs to PHGG microparticles was possible. The values of association efficiency and loading capacity are displayed in Table 4.2.

Table 4.2 – Drug association efficiency (AE) and microparticle loading capacity (LC) of PHGG-based microparticles (Mean ± Standard deviation, n = 3).

Formulation	AE (%)	LC (%)
PHGG:Man:INH	63.3 ± 1.5	6.33 ± 0.15
PHGG:RFB	67.8 ± 1.1	6.78 ± 0.11
PHGG:INH:RFB	65.0 ± 3.3 (INH) 57.2 ± 7.9 (RFB)	6.06 ± 0.4 (INH) 5.72 ± 1.2 (RFB)

A previous test confirmed that the polysaccharide did not interfere with drug signals at the established wavelengths. The association efficiency of drugs varied roughly between 50% and 70% and was considered to occur with approximate effectiveness both when the drugs were associated individually or in combination, with a small difference observed for RFB. In fact, when comparing microparticles with each of the drugs individually with the formulations of drug combination, it is observed that the association of INH did not vary significantly, but the association of RFB decreased ($P < 0.05$) approximately 10% (comparison of mean values). The literature does not provide data on spray-dried guar gum based microparticles associated with INH or RFB. However, for chitosan for instance, which is the most common polysaccharide being used in drug delivery, association efficiencies around 80% are usually reported [44, 72]. In the Grenha's lab other formulations of polysaccharide-based microparticles are under development, using other polymers (carrageenan, locust bean gum, glucomannan) but the same antitubercular drugs. The observed results are variable regarding the ability to associate the drugs. Locust bean gum microparticles, for example, associate RFB (alone) with 100% efficiency [76], but in the case of carrageenan microparticles associating both drugs, the results were much more similar (74% for INH and 57% for RFB) [77] with those reported in this thesis. In a general manner, although with some exceptions, it was verified that PHGG formulations associated INH with efficiency approximately similar to other formulations developed by the team having a different polysaccharide composition. In turn, that was not the case for RFB, as lower association efficiency was generally observed in this work. The explanation for that effect is possibly related with the used amount of HCl. All formulations having RFB require the use of HCl for solubilization of the antibiotic, although different concentrations of HCl might be used in different works (that is, for different polysaccharides). PHGG microparticles were prepared using HCl 0.001M, but other formulations used higher concentrations (up to 0.1M). A lower concentration of HCl does not allow as much protonation of rifabutin and perhaps in that way

weaker interactions were established with the polymer, thus resulting in lower association of the drug.

Regarding the loading capacity, it ranged within 6-7%, which is in line with some reports on the literature for inhalable antibiotics that affirm that the drug is often less than 10% loading, with an average of about 5% [74]. It is important to mention that establishing comparisons with results available on the literature was quite a difficult task due to a wide variation of polymer/drug ratios, which results in a disparity of values.

4.4. *In vitro* drug release profile

The drug release profile is an important parameter to characterize in the development of a drug delivery system. The drug release rate is reported to depend on the solubility of the free drug, its desorption from the surface, drug diffusion on the microparticle matrix, microparticle matrix degradation, and combination of degradation/diffusion processes [73]. Maintaining sink conditions requires keeping the drug concentration in the release medium low enough not to affect the concentration gradient for drug release. This could be a challenge if the drug is hydrophobic, so it is recommended that the drug concentration must be kept below 30% of saturation to maintain sink conditions [78]. Figure 4.7 depicts the release profile of RFB from PHGG:RFB microparticles and Figure 4.8 that of both INH and RFB from PHGG:INH:RFB microparticles in a medium composed by PBS pH 7.4 and Tween® 80. This medium was used in order to mimic the lung environment that microparticles are expected to find after inhalation and reaching of alveolar zone. PBS has a pH resembling that of lung lining fluid, which is reported to be around 7 [79]. Additionally, the alveolar zone counts with the presence of lung surfactant, which is composed of 80% phospholipids [80]. Tween® 80 was added to resemble this content of tensioactive substances. In parallel, its presence is beneficial for the solubilization of the hydrophobic RFB, thus enabling the performance of the release assays in proper conditions.

In both tested formulations, the release of RFB was in general quite fast, as approximately 80% - 90% of the drug is released in 15 minutes. However, during the first 15 minutes the release is progressive, an effect that is not observed for INH. For the latter drug, 75% of drug is already quantified after 5 minutes.

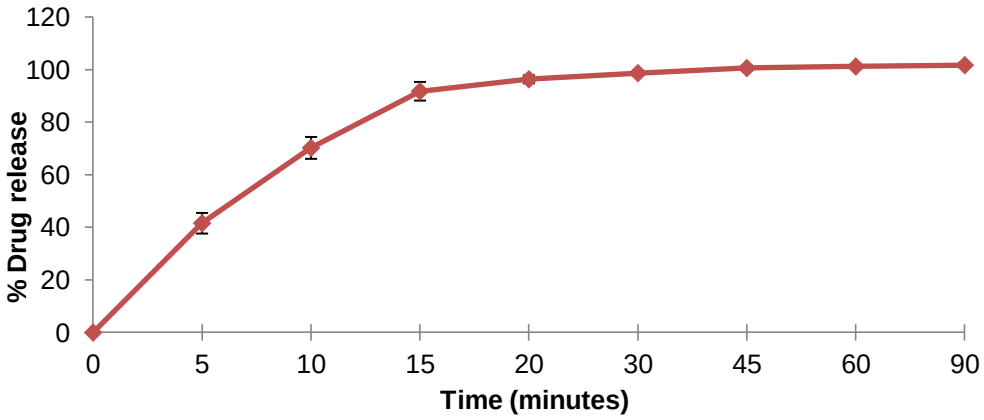

Figure 4.7 – RFB release profile from PHGG:RFB microparticles in PBS/Tween®, at 37 ºC (Mean ± Standard deviation, n = 3).

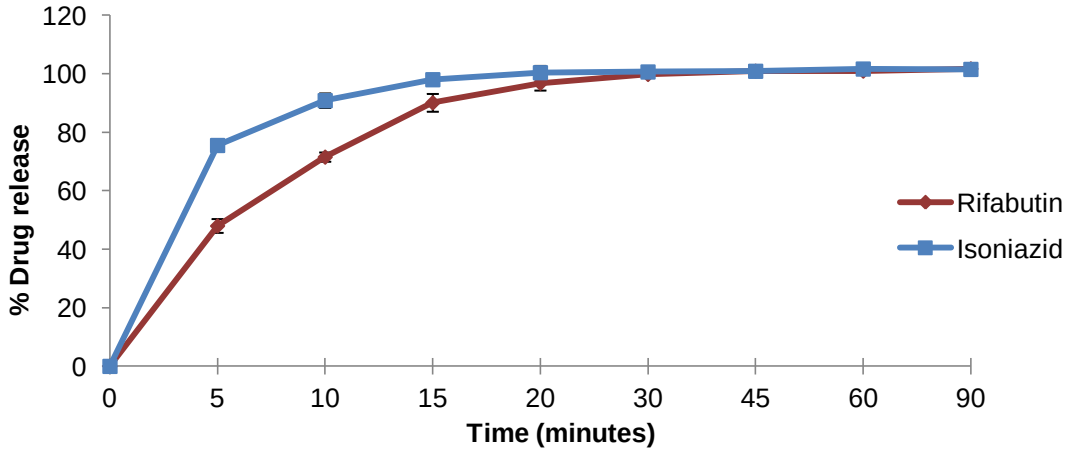

Figure 4.8 – INH and RFB release profile from PHGG:INH:RFB microparticles in PBS/Tween®, at 37 ºC (Mean ± Standard deviation, n = 3).

The rate of RFB release is thus a little slower than that of INH, which is probably related with the higher aqueous solubility of INH. In both formulations, the maximum release of RFB was achieved at approximately 30 minutes, while that of INH was registered around 15 minutes.

The release from the formulation PHGG:Man:INH was not determined in this thesis, because it was characterized in a previous work of the group. Although in that case the referred assay was performed using only PBS pH 7.4 as release medium, no Tween® being included, the release was also very rapid (100% in 20 minutes, data not shown). In fact, owing to the high solubility of INH, the presence of Tween® is not expected to have a significant effect on the release rate. As a whole, the reason for the rapid release of the drugs is mainly attributed to the fact that the medium is hydrophilic and the matrix of the microparticles is highly soluble, due to its exposed hydroxyl groups.

4.5. Evaluation of microparticle cytotoxicity

Evaluating the cytotoxic profile of drug formulations is a relevant parameter in the development of any therapeutic strategy. Several tests can be performed to do this evaluation and in this thesis two different assays were selected, which focus cell metabolic activity (MTT assay) and cell membrane integrity (LDH release assay) [81]. The MTT assay is often used, although it has the limitation of not permitting a clear differentiation between cell cycle inhibition and cellular death. The LDH release assay is often applied complementarily and involves the quantification of a cytoplasmic enzyme which only releases to cell culture medium if cell membrane is damaged [82].

The assays were conducted on three cells lines. Two are respiratory carcinoma cell lines representative of the bronchial and alveolar epithelia, Calu-3 and A549 cells, respectively. These are very similar from a physiological point of view, although A549 cells do not form confluent and tight monolayers. In particular, Calu-3 cells present high similarity to *in vivo* physiology [83]. Regarding the purpose of this thesis, the A549 cells will be those providing perhaps the most relevant information on cytotoxicity, as the formulations are designed and expected to reach the alveolar zone in high amounts. However, Calu-3 cells are also relevant, because it is known that there is always a certain amount of dry powder depositing in the bronchial area. The third cell line consists of THP-1 cells differentiated to macrophage-like cells, which were used to provide indications on the cytotoxicity of formulations towards alveolar macrophages, which are the targets of the developed therapeutics.

4.5.1. MTT assay

Figure 4.9 represents the cell viability obtained for INH and RFB at different concentrations, at the end of 3 and 24 hours exposure to A549 cells. Extending the assays until 24 hours is a relevant issue, because it represents the clearance time of foreign substances from the lung [84].

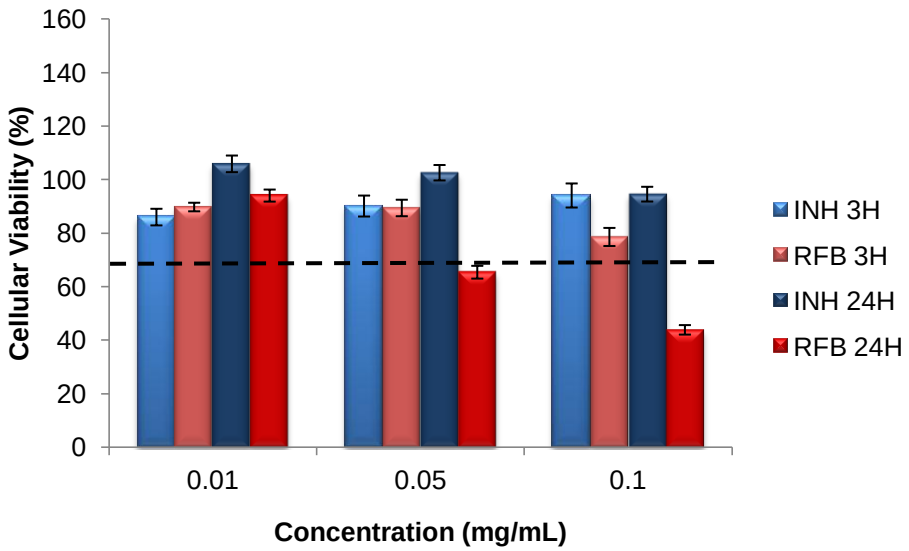

Figure 4.9 – Cell viability of A549 cells, after 3 and 24 hours of incubation with antitubercular drugs INH and RFB (Mean ± SEM, n = 3). Dotted line indicates 70%.

Drug concentrations ranged between 0.01 and 0.1 mg/mL, approximately corresponding to the amounts present in drug-loaded microparticles. Considering that drugs were associated to microparticles at a polymer/drug mass ratio of 10:1, the amount of drug is approximately 10% that of the total mass. As the formulations were tested at the concentrations of 0.1, 0.5 and 1 mg/mL, drug concentrations representing 10% of that were those selected to be assessed (0.01, 0.05 and 0.1 mg/mL). Results from the figure indicate an absence of toxic effect for a contact time of 3 hours, as cell viability remains above 70% in all tested conditions and that is the value established by ISO 10993 below which toxic effects are considered to occur [85]. Regarding INH, it induces cell viability between 80% and 100% in all occasions, either at 3 or 24 hours. The scenario changes upon exposure to RFB, which has a clear concentration- and time-dependent behavior. While at 3 hours no significant cytotoxicity is observed, upon 24 hours exposure a cytotoxic effect appears ($p < 0.05$). For that exposure time, the concentration of 0.05 mg/mL already results in cell viability a little below 70%, and the value decreases to 44% for 0.1 mg/mL of RFB ($p < 0.05$). This indicates that cell metabolism is highly inhibited in the presence of higher concentrations of this drug. Figure 4.10 also depicts cell viability obtained upon exposure to INH and RFB, but in Calu-3 cells.

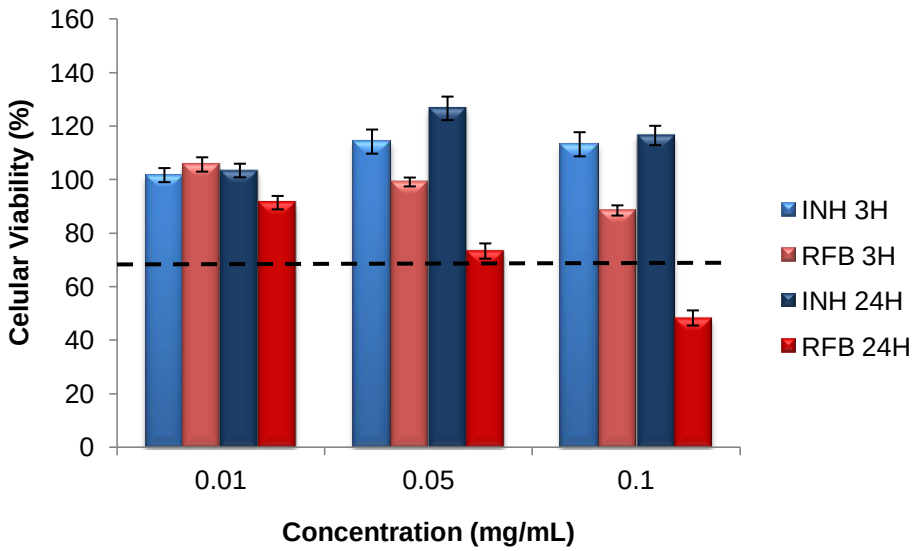

Figure 4.10 – Cell viability of Calu-3 cells, after 3 and 24 hours of incubation with INH and RFB (Mean ± SEM, n = 3). Dotted line indicates 70%.

Although with some variations, the comparison of these results with those obtained on A549 cells reveals the same trend. In fact, at 3 hours no cytotoxic effect is observed (cell viability above 70% in all cases), INH does not decrease cell viability to significant levels even upon 24 hours incubation and, finally, RFB induces both a time- and concentration-dependent effect ($p < 0.05$). Regarding the latter, while at 3 hours no decrease in cell viability is observed beyond the threshold of 70%, upon 24 hours a strong decrease is registered, reaching its minimum for the concentration of 0.1 mg/mL (48%, $p < 0.05$). Regarding the most detrimental condition (RFB exposure for 24 hours at 0.1 mg/mL), the resultant cell viability is very similar between the two cells lines. It is interesting to note that the incubation with INH resulted in some cases in cell viability well above 100%. This effect has been reported in the literature upon contact with some substances such as saccharides [79, 84]. Additionally, a similar non-cytotoxic effect towards different respiratory cell lines, at concentrations below 2.5 mg/mL, was reported for free INH and INH-proliposome formulation [65]. Figure 4.11 represents the corresponding results for macrophage-like cells (differentiated THP-1 cells). These cells are apparently less sensitive than the other two cells lines, as more amenable effects were observed. In fact, all conditions resulted in cell viability above 70%, with the exception of that of RFB incubated for 24 hours at the higher concentration tested (0.1 mg/mL). Even in that case, cell viability was of 60%, thus reflecting a less pronounced effect. Again, RFB has shown a time- and concentration-dependent effect ($p < 0.05$).

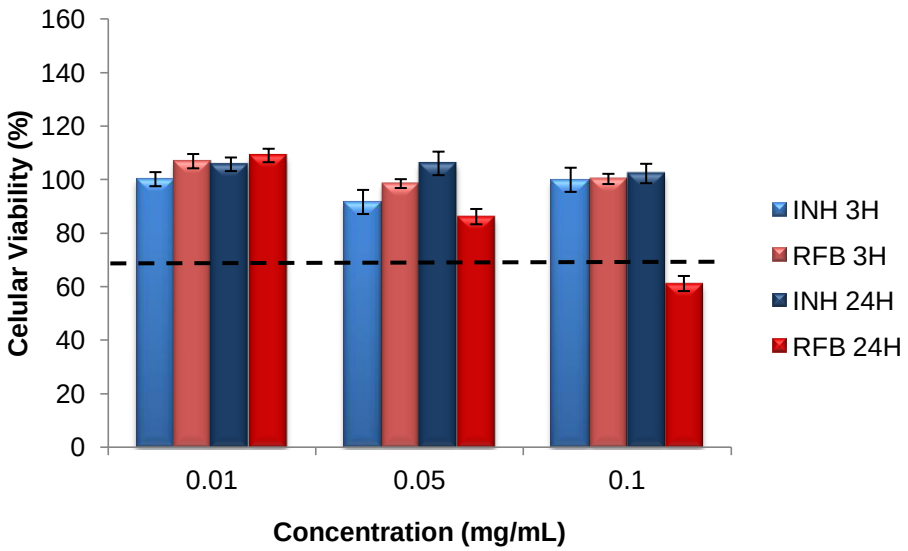

Figure 4.11 – Cell viability of macrophage-like cells, after 3 and 24 hours of incubation with INH and RFB (Mean ± SEM, n = 3). Dotted line indicates 70%.

Apart from testing the free drugs, it is of relevance to determine the effect of the materials composing the matrix of the developed microparticle formulations. In this manner, the three cell lines were also exposed to the presence of PHGG as obtained commercially, PHGG after spray-drying and the spray-dried mixture of PHGG and mannitol (PHGG:Man). Results obtained upon 24 hours exposure in macrophage-like cells (derived from THP-1 cells) are depicted in Figure 4.12. This figure is considered representative of what occurred in the other two cell lines, as cell viabilities remained very close to 100% in almost all cases (and never decreased from 80%), independently of the cell line being used. Figures depicting the results of other assay times and cell lines are available in Chapter VII – Annexes.

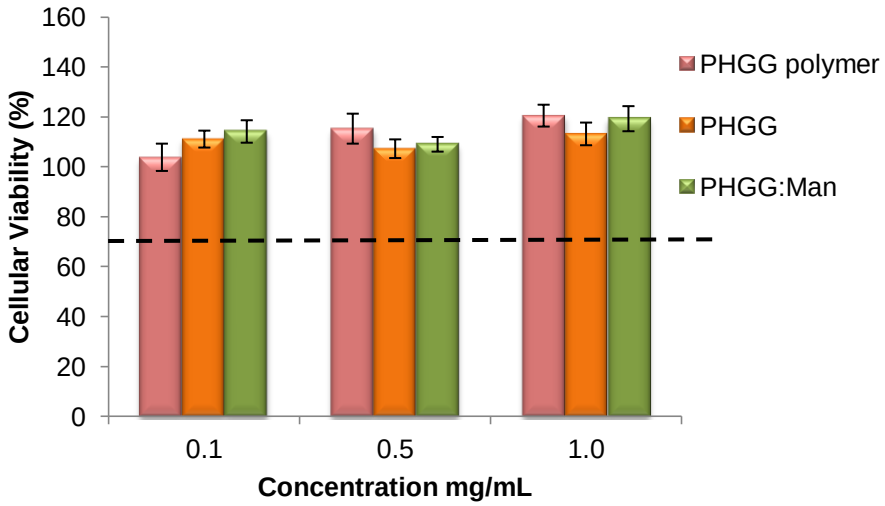

Figure 4.12 – Cell viability of macrophage-like cells (differentiated THP-1 cells), after 24 hours of incubation with PHGG polymer, spray-dried PHGG and PHGG:Man microparticles (Mean ± SEM, n = 3). Dotted line indicates 70%.

Drug-loaded formulations were also tested in all three cell lines. Figure 4.13 shows the results for A549 cells.

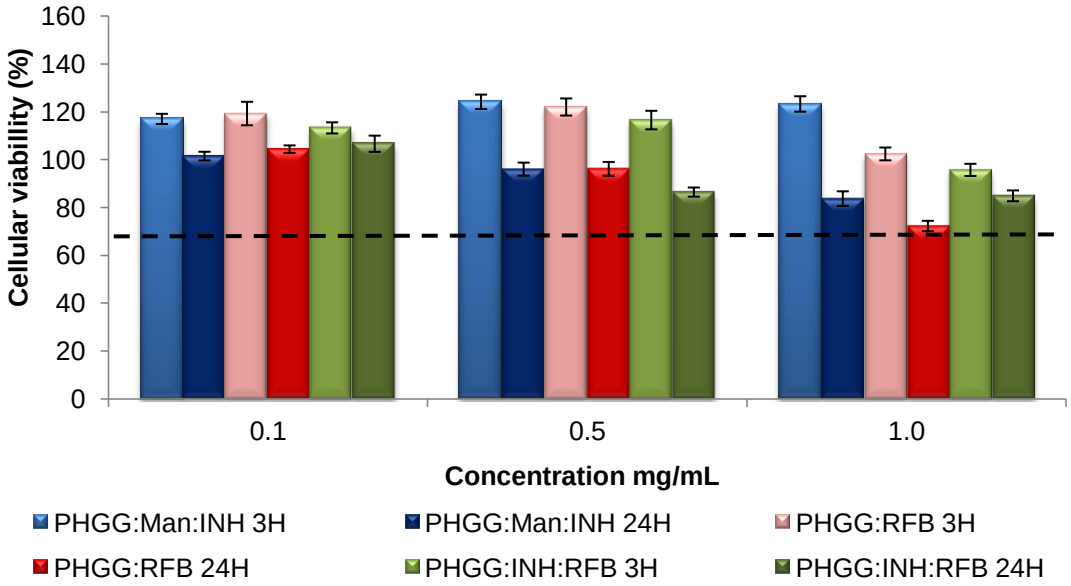

Figure 4.13 – Cell viability of A549 cells, after 3 and 24 hours of incubation with PHGG:Man:INH, PHGG:RFB and PHGG:INH:RFB microparticles (Mean ± SEM, n = 3).

Microparticles loaded with INH, RFB or both drugs do not display cytotoxicity for the concentrations of 0.1 and 0.5 mg/mL, either at 3 or 24 hours. Upon 24 hours exposure some decrease on cell viability was observed at the concentration of 1 mg/mL, but the lowest cell viability value was of 72% (PHGG:RFB), thus being devoid of physiological relevance. Considering that RFB analyzed as free drug has shown great toxicity at the same conditions (44% cell viability), the plausible explanation for these cell viability results of RFB-loaded microparticles is the not so high association efficiency of RFB (around 60%). Taking this into

account, the real amount of RFB in microparticles will be more equivalent to the concentration of 0.05 mg/mL than to 0.1 mg/mL. The former induced in A549 cells viability above 60%, thus in line with what is obtained for RFB-loaded formulations.

Calu-3 cells revealed a similar trend of response to the exposure of drug-loaded PHGG microparticles (Figure 4.14). As observed, in no case does cell viability decrease below 70%. Although in some cases cell viability decreases to a significant statistical level, as for the incubation with RFB-loaded microparticles either alone or in combination with INH, after 24 hours at 1.0 mg/mL ($p < 0.05$), cell viability is still considered very acceptable (> 80%).

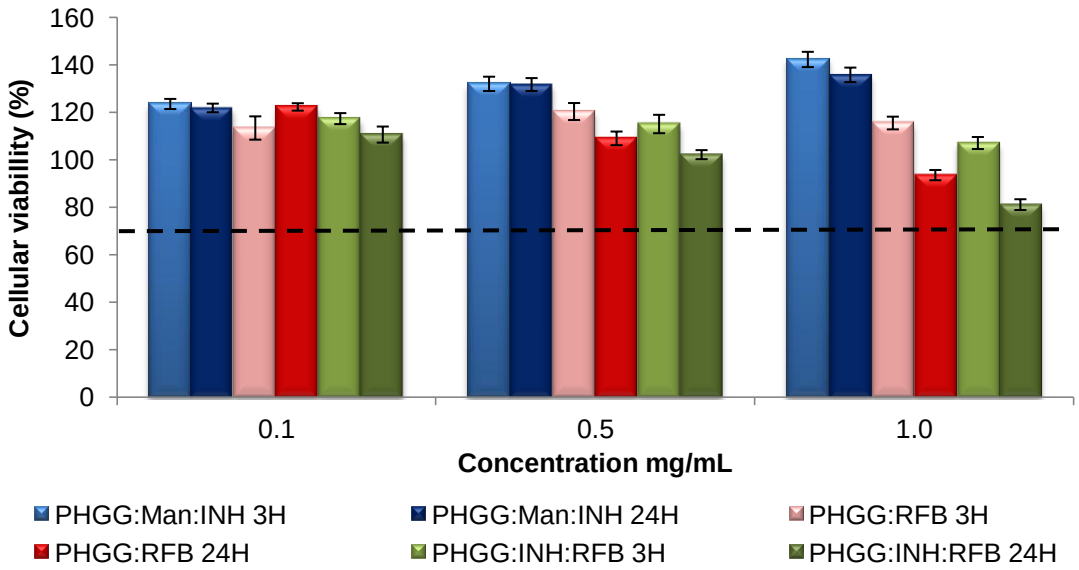

Figure 4.14 – Cell viability of Calu-3 cells, after 3 and 24 hours of incubation with PHGG:Man:INH, PHGG:RFB and PHGG:INH:RFB microparticles (Mean ± SEM, n = 3). Dotted line indicates 70%.

The results obtained for macrophage-differentiated THP-1 cells also generally followed the trend exposed for the other cell lines, as no overt toxicity was detected and cell viability values were above 70% (Figure 4.15).

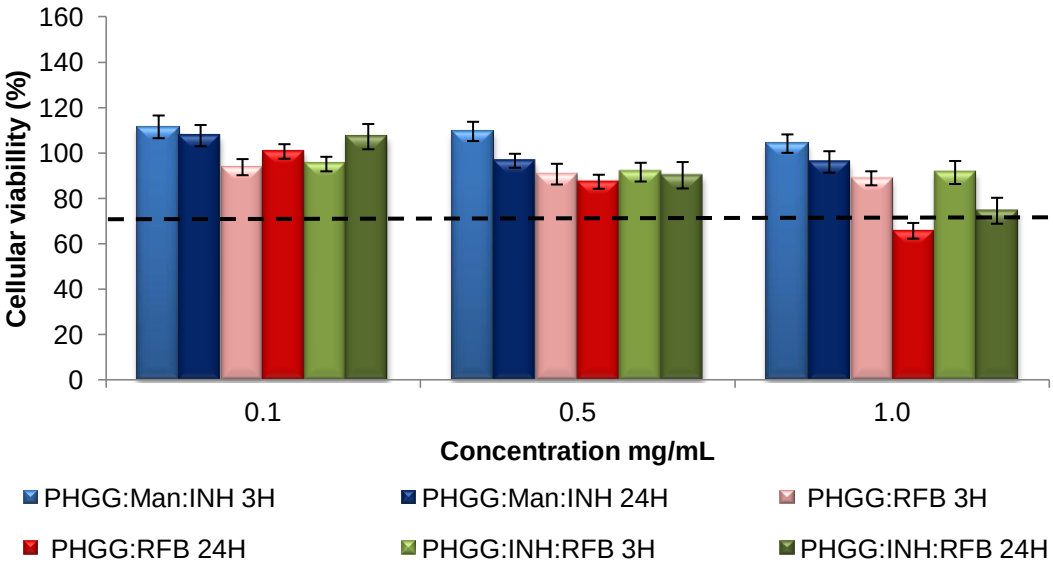

Figure 4.15 – Cell viability of macrophage-differentiated THP-1 cells, after 3 and 24 hours of incubation with PHGG:Man:INH, PHGG:RFB and PHGG:INH:RFB microparticles (Mean ± SEM, n = 3). Dotted line indicates 70%.

The lower cell viabilities were found at the concentration of 1 mg/mL, but only the exposure to PHGG:RFB microparticles for 24 hours induced a value below 70%, more precisely 66%. The fact that only in this cell line the viability decreased below 70% for this formulation might be related with the fact that PHGG is composed of mannose units which are favorably recognized by macrophage mannose receptors. Therefore, microparticles have possibly a stronger interaction and internalization with these cells, which results in increased toxicity.

4.5.2. LDH assay

As stated in the methodology section, the LDH assay provides a quantification of the cytoplasmic enzyme LDH released to the supernatant of cells upon exposure to a potential toxicant. Based on the results obtained on the MTT assay, the free drugs and microparticle formulations were evaluated for an exposure of 24 hours at the higher concentrations tested (0.1 mg/mL for drugs and 1 mg/mL for microparticles). An assessment of RFB as free drug at the concentration of 0.05 mg/mL was also performed due to the higher toxicity induced by this drug.

Figure 4.16 shows the results obtained upon exposure of the three cell lines to free drugs. The amount of LDH released by cells incubated with culture medium only was assumed as 100% LDH release, so any result above that value indicates a certain level of cell membrane damage.

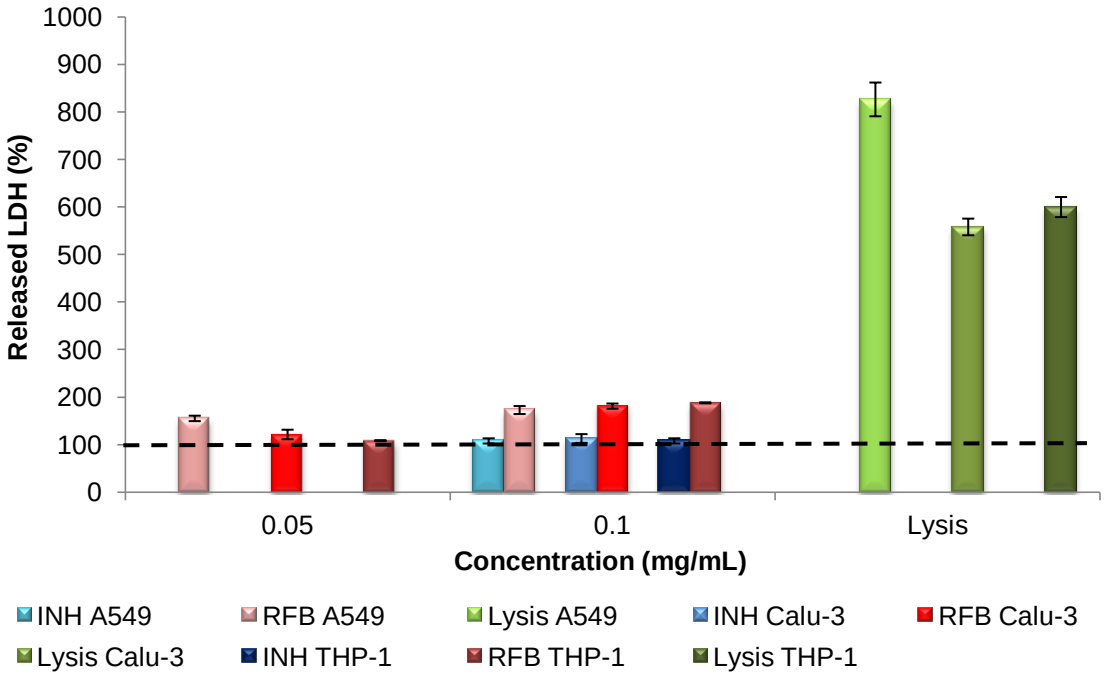

Figure 4.16 – Released LDH (%) upon exposure of A549, Calu-3 and differentiated THP-1 cells to INH and RFB drugs at different concentrations (Mean ± SEM, n = 3). Dotted line represents 100% LDH release.

The contact with INH induces in all cases a result similar to that of the control, as all values are around 100 – 110%. The exposure to RFB at 0.05 mg/mL showed a significantly higher release of LDH in A549 cells (155%, $p < 0.05$) and also in Calu-3 cells, although in this case a much lower amount was registered (121%, $p < 0.05$). These results demonstrate again that THP-1 cells are more robust and A549 cells the most sensitive of the three. At the concentration of 0.1 mg/mL, RFB induced stronger increase in released LDH ($p < 0.05$), with values between 170% and 190% in all cell lines. There are significant differences between RFB concentrations, evidencing that the cytotoxic effects are dose-dependent ($p < 0.05$). However, the LDH release induced by incubation with the drugs is in all cases much lower ($p < 0.05$) that that induced by the lysis buffer, inducing values between 550% and 830%. The results generated by exposure to RFB as free drug are considered in line with those obtained in the MTT assay, as the 24 hour incubation with 0.1 mg/mL RFB also resulted in a considerably detrimental effect to the cells independently of the cell line.

The assessment of the unloaded microparticles and drug-loaded microparticles demonstrated to be in line with previous findings. In fact, PHGG polymer as obtained commercially or in the form of spray-dried microparticles, and PHGG microparticles containing the adjuvant excipient mannitol, registered LDH release values around 100% when exposed to A549 cells, not evidencing any damaging potential (Figure 4.17).

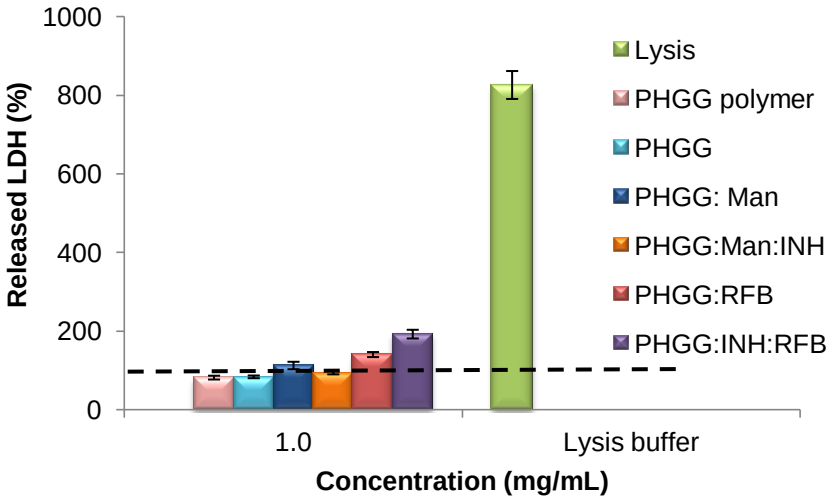

Figure 4.17 – Released LDH (%) upon A549 cell exposure for 24 hours to PHGG microparticles containing or not INH and RFB, at the concentration of 1 mg/mL (Mean ± SEM, n = 3). Dotted line represents 100% LDH release.

The association of INH to the microparticles did not induce any alteration, demonstrating again an absence of cytotoxicity of this antibiotic. In turn, the incorporation of RFB, either alone or in combination with INH, was found to increase the released LDH ($p < 0.05$) to 141% and 168%, respectively.

Calu-3 cells displayed a similar profile (Figure 4.18), but possibly because of their robustness as compared with A549 cells, the observed effects were less pronounced.

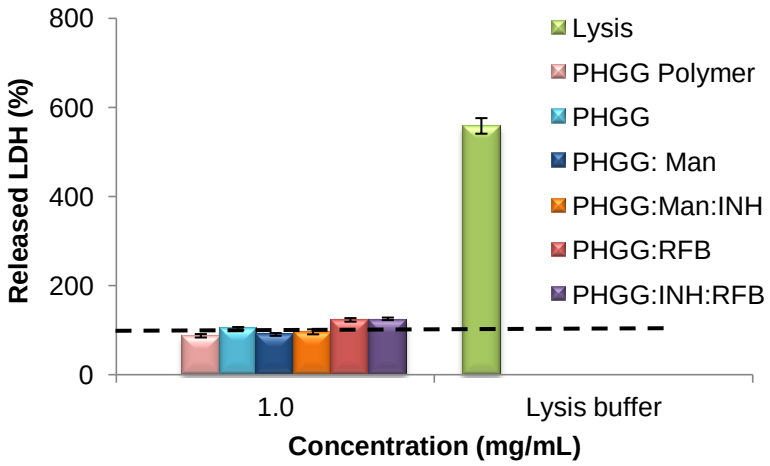

Figure 4.18 – Released LDH (%) upon Calu-3 cell exposure for 24 hours to PHGG microparticles containing or not INH and RFB, at the concentration of 1 mg/mL (Mean ± SEM, n = 3). Dotted line represents 100% LDH release

The exposure of these cells to PHGG polymer, PHGG microparticles, PHGG:Man and PHGG:Man:INH microparticles, resulted in LDH release varying within 86% and 103%, thus not indicating any membrane damaging potential. Microparticle formulations containing RFB (PHGG:RFB and PHGG:INH:RFB microparticles) resulted in values around 120%, which although statistically significant different ($p < 0.05$) are not as strong as those found in A549

cells, the effect being considered mild. Finally, a rather different response to the RFB-loaded microparticles was found for macrophage-differentiated THP-1 cells. As depicted in Figure 4.19, unloaded or INH-loaded microparticles result in values quite close to 100%, being devoid of toxicity, but the exposure to microparticles containing RFB resulted in LDH release exceeding 200% (228% for PHGG:RFB and 230% for PHGG:INH:RFB)..

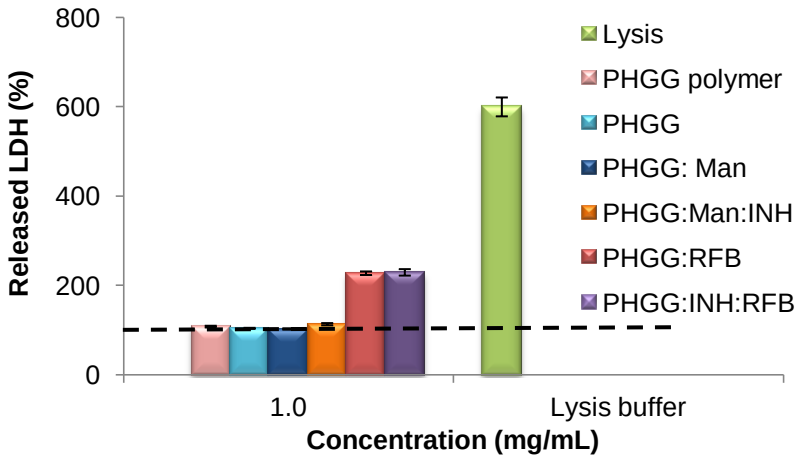

Figure 4.19 – Released LDH (%) upon 24 hours exposure of macrophage-differentiated THP-1 cells to PHGG microparticles containing or not INH and RFB, at the concentration of 1 mg/mL (Mean ± SEM, n = 3). Dotted line represents 100% LDH release.

These values are of statistical significance ($p < 0.05$) and evidence strong toxicity against these cells. In this case, the results are not in line with those obtained in the MTT assay, as the present assay indicates a much higher level of toxicity. Based on the literature, the use of PMA induces a certain cell cycle arrest following by THP-1 cell differentiation [87], conditioning the results based on the MTT assay, since it is not as sensitive as LDH.

4.6. The susceptibility of *M. smegmatis*

The MIC values for INH, RFB and associated drugs against *M. smegmatis* (Figure 4.20) were determined. The same determination was then performed for the MPs PHGG:INH, PHGG:RFB and PHGG:INH:RFB, using the MTT and recovery drop methods, as previously mentioned (section 3.9 from Materials and Methods). In Table 4.3 is shown the MIC value for MPs with INH, RFB and associated drugs.

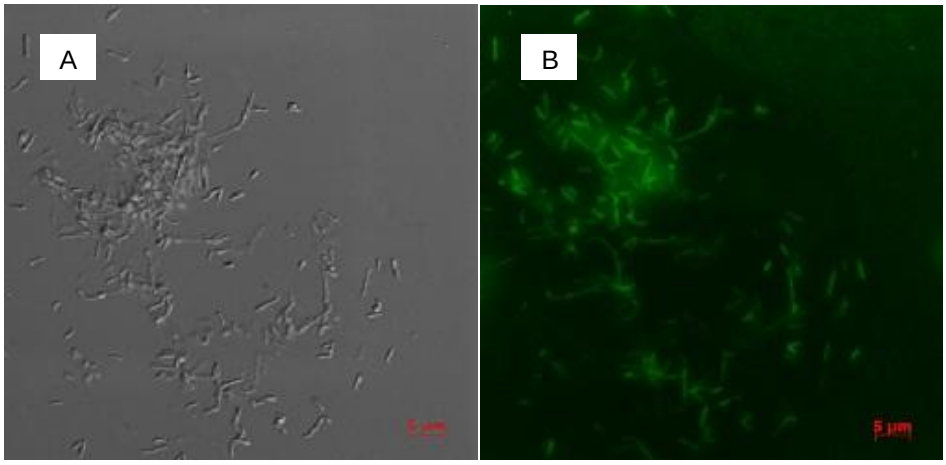

Figure 4.20 – *M. smegmatis* cells observed A) by differential interference contrast, B) by fluorescence (bacterial cells were stained with Live/Dead Molecular Probes (Invitrogen). (Scale: 5 μm).

Table 4.3 – Viability (%) of *M. smegmatis* exposed to different concentrations (16-0.25 μg/mL) of MPs with INH, RFB (0.8-0.025 μg/mL), and both drugs INH and RFB (2-0.015 μg/mL) as determined by the MTT test. Data represent mean ± Standard deviation of three replicates per 2 wells (n = 6).

MPs loaded with INH							
Control culture	32	16	8	4	2	1	0.5
98.4±9.9	18.0±5.4	16.3±2.8	19.6±5.7	27.2±8.5	84.0±11.5	108.8±10.4	113.9±12.4

MPs loaded with RFB						
Control culture	0.8	0.4	0.2	0.1	0.05	0.025
100.8±8.1	10.2±8.4	12.0±3.0	34.6±9.3	63.7±4.3	75.5±6.2	89.7±5.6

MPs loaded with INH and RFB								
Control culture	2	1	0.5	0.25	0.125	0.06	0.03	0.015
97.1±17.1	7.0±9.0	38.5±5.9	73.9±9.9	113.3±7.2	110.6±2.1	102.7 ±8.6	127.0 ±9.2	130.1±7.7

The MIC value for INH drug against *M. smegmatis* was 4 μg/mL, which is similar to the previous MIC value reported by Wang and Marcotte (2008) [21]. The data retrieved from the MTT plates showed that the mean value for bacterial growth with the presence of 4 μg/mL of INH drug was 27.2 ± 8.5% viability, turning to 84.0 ± 11.5% on the following concentration (2 μg/mL). The same MIC value was observed by recovery drops in agar plates, where a few colonies still persisted, but the majority was inhibited. This MIC value suggests that this strain of *M. smegmatis* shows resistance to INH, and might carry a mutation on *katG* gene or in other genes [88]. The MIC value for MPs could have been lower than for the INH drug, because the drug association percentage (AE%) was below 100%, serial two fold dilutions should have been done with different values between 4 and 2 μg/mL. The RFB MIC value for *M. smegmatis*, determined by the MTT test and confirmed by recovery drops, was 0.2 μg/mL, at which

concentration was achieved a 34.6± 9.3% viability, following at the next concentration a viability value of 63.7 ± 4.3 %. Our RFB MIC value is similar to the previously reported, that was 0.25 μg/mL [89]. Such slightly differences on the RFB MIC value may be related with the strain and the different methodology used. The determined MIC for both drugs was 1 μg/mL. Analyzing the data retrieved from Table 4.3, the viability of *M. smegmatis* in the presence of 1 μg/mL of both drugs was 38.5 ± 5.9%, turning to 73.9 ± 9.9% on the following concentration (0.5 μg/mL). This MIC value seems to be accurate, because it is comprehended between 4 and 0.2 μg/mL, respective MIC values for INH drug and MPs loaded with INH; RFB drug and MPs loaded with RFB alone, correspondingly.

4.7. The susceptibility of *M. bovis*

The MIC values were determined for the MPs PHGG:INH and PHGG:RFB using the MTT test. In Table 4.4 the MIC value for MPs loaded with INH and with RFB against *M. bovis* is shown.

Table 4.4 – Viability (%) of *M. bovis* exposed to different concentrations (1-0.015 μg/mL) of MPs with INH, and with RFB (1-0.015 μg/mL), determined by the MTT assay. Data represent Mean ± Standard deviation of three replicates per 2 wells (n = 6).

MPs loaded with INH							
Control culture	1	0.5	0.25	0.125	0.06	0.03	0.015
93.7±10.9	18.5±9.4	21.1±2.6	27.1±5.6	28.5±3.4	87.2±5.1	91.5±9.4	103.0±4.7
MPs loaded with RFB							
Control culture	1	0.5	0.25	0.125	0.06	0.03	0.015
91.5 ± 15.1	11.5±3.6	18.0±4.2	23.9±3.3	21.8±4.4	22.5±5.4	73.5±9.8	92.1±10.8

For the MPs loaded with INH, MIC value for *M. bovis* was 0.125 μg/mL, at which concentration was achieved a 28.5 ± 3.4% of viability, following at the next concentration a viability value of 87.17 ± 5.13%. This MIC value is similar to the *M. bovis* BCG-Connaught strain previously reported by Ritz *et al* (2009) [90]. The MIC value of MPs with RFB for *M. bovis* was 0.06 μg/mL at which concentration achieved 22.5 ± 5.4% viability following, at the following concentration a viability value of 73.5 ± 5.4%. The same MIC value has been observed in several strains of *M. bovis* BCG [90].

Due to time consuming growth conditions and material delay, it was not possible to determine the MIC value for MPs with the combination of drugs, thus the hypothetically MIC value should have ranged between 0.125 and 0.06 μg/mL (≈ 0.08 μg/mL). Additionally, the MIC values of free drugs should have been determined in order to compare the susceptibility of *M.bovis* with the antitubercular free drugs, and in contact with the MPs.

The *M. bovis* strain displayed MIC values lower than the ones displayed by *M. smegmatis*, which implies that *M. bovis* is more susceptible to these antitubercular drugs than *M. smegmatis*. Since *M. bovis* is highly pathogenic showing a susceptibly level of few μg/mL of the evaluated antitubercular drugs, shows that a theoretical therapeutic approach may require low concentration doses to eliminate *M. bovis* infection.

4.8. Therapeutic effectiveness *in vitro*

The assay of *in vitro* infection of macrophage-like cells with *M. smegmatis* was conducted during 4 and 24 hours. Table 4.5 shows the viability of the intracellular *M. smegmatis* exposed to free drugs and MPs with both drugs, after 4 and 24 hours of infection.

Table 4.5 – Viability (%) of control, *M. smegmatis* exposed to associated free drugs (MIC = 1 μg/mL), and with MPs with both drugs (MIC = 1 μg/mL). Data represents the Mean ± Standard deviation of three replicates for each plate (n = 6).

	Control (No drugs added)	Free drugs INH and RFB	MPs with both drugs
M. smegmatis viability (%) after 4 h exposure	110.5 ± 3.0	62.2 ± 10.5	27.6 ± 6.0
M. smegmatis viability (%) after 24 h exposure	51.1 ± 7.3	46.0 ± 7.1	22.5 ± 9.6

After 4 hours exposure of *M. smegmatis* to the free drugs the mycobacterial viability was reduced to 62.2 ± 10.5%, in contrast to the exposure to the MPs with both drugs that caused a viability reduction of 27.6 ± 6.0%. The control culture after 4 hours achieved 110.5 ± 3.0% of viability.

These results suggest that microparticles loaded with both drugs, effectively targeted the macrophage-like cells, possibly mediated by the mannose and galactose receptors. This effect of MPs on the mycobacterial viability is promising in the elimination of the intracellular pathogen in comparison to the free drugs.

After 24 hours of infection in the presence of free drugs the mycobacterial viability was 46.0 ± 7.1%, in contrast to the exposure to MPs with both drugs, for which a viability of 22.5 ± 9.6% was observed. The control culture showed a 51.1 ± 7.3% of viability after the same time interval. The latter reduction on the viability of intracellular *M. smegmatis* cells is possibly related with the absence of antiphagocytic mechanisms in this species, as is observed for *M. tuberculosis*. Nevertheless, it is important to stress that after the same time interval, the action of MPs against *M. smegmatis* reached almost a double reduction of the mycobacterial population, in comparison to the free drugs. Altogether, these results highlight the potential use of MPs loaded with antitubercular drugs to control mycobacterial infections.

The infection of macrophage-like cells with *M. bovis* was not possible to perform, due to time constraints. Considering the pathogenicity of this strain, the assay would have been more representative of the processes occurring with MTB.

Chapter V – Conclusions

This thesis proposes a novel therapeutic approach to tuberculosis, based on pulmonary drug delivery of antitubercular drugs. Spray-dried PHGG microparticles proved to present suitable properties for lung delivery in the ambit of tuberculosis therapy. The microparticles successfully encapsulated isoniazid and rifabutin, two first-line antitubercular drugs, either alone or

combined, in all cases with efficiencies between 55% and 70%. The release of drugs in a medium resembling the alveolar environment was rapid (100% RFB at 30 minutes and at 15 minutes for INH), owing to the hydrophilic character of PHGG. A lack of overt toxicity was generally observed for all developed drug-loaded microparticle formulations by the MTT assay in conditions involving up to 24 hours exposure and concentrations varying between 0.1 and 1 mg/mL. Three cell lines representing the respiratory area and relevant for the work were used (alveolar A549, bronchial Calu-3 and macrophage-differentiated THP-1 cells) and cell viabilities did not decrease below 66%. The lower cell viability values corresponded to RFB-containing microparticles. However, the LDH release assay revealed considerable degree of cell membrane damage in certain cases, particularly for formulations containing RFB. The *in vitro* response of macrophages infected with *Mycobacterium smegmatis* to the presence of drug-loaded PHGG microparticles was favorable regarding the elimination of bacteria. The incubation of infected macrophages with PHGG/INH/RFB microparticles reduced the infection level to around 20% in 24 hours, comparing with 46% obtained for free combined drugs. Taking into account the whole set of results, it seems adequate to assume that PHGG microparticles are suitable vehicles of antitubercular drugs to be proposed as an alternative inhalable therapeutic approach to lung tuberculosis therapy.

Chapter VI – Bibliography

[1] Gomes, M. J. P. "Gênero Mycobacterium spp." *Favet-Ufrgs* 1 – 90 (2013).

[2] De Backer, A. I., Mortelé, K. J., De Keulenaer, B. L. & Parizel, P. M. "Tuberculosis: epidemiology, manifestations, and the value of medical imaging in diagnosis." *JBR-BTR* **89,** 243–250 (2006).

[3] Medcalf, A., Altink, H., Saavedra, M. and Bhattacharya, S. "Tuberculosis - A short story." *Univ. York* (2013).

[4] Tripathi, R. P., Tewari, N., Dwivedi, N. & Tiwari, V. K. "Fighting tuberculosis: an old disease with new challenges." *Med. Res. Rev.* **25,** 93–131 (2005).

[5] Costa, H. & Grenha, A. "Natural carriers for application in tuberculosis treatment." *J. Microencapsul.* **30,** 1–12 (2012).

[6] Misaki, W. & Byarugaba, W. "Emphasizing the vitality of genomics related research in the area of infectious diseases." *Sci. Res. Essay* **3,** 125–131 (2008).

[7] WHO. "Global tuberculosis report 2014." *WHO/HTM/TB/2014.08. World Heal. Organ. Geneva* (2014).

[8] Ranjita, S., Shaal, A. & Khalil, M." Present Status Tuberculosis of Nanoparticle for Treatment of Tuberculosis". *J Pharm Pharm. Sci* **14,** 100–116 (2011).

[9] Whiteford, D. "Stress survival in *Mycobacterium tuberculosis* and *Mycobacterium bovis* and the role of hup in *Mycobacterium smegmatis*." *Washingt. State Univ.* (2008).

[10] Ahmad, S. "Pathogenesis, immunology, and diagnosis of latent *Mycobacterium tuberculosis* infection." *Clin. Dev. Immunol.* **2011,** (2011).

[11] Chan, J. G. Y. *et al.* "A novel dry powder inhalable formulation incorporating three first-line anti-tubercular antibiotics." *Eur. J. Pharm. Biopharm.* **83,** 285–292 (2013).

[12] Welin, A. "Survival strategies of Mycobacterium tuberculosis inside the human macrophage." *Linkonping Univ.* (2011).

[13] Gupta, A., Kaul, A., Tsolaki, A. G., Kishore, U. & Bhakta, S. *Mycobacterium tuberculosis*: Immune evasion, latency and reactivation. *Immunobiology* **217,** 363–374 (2012).

[14] Flynn, J. L. & Chan, J. "Tuberculosis : Latency and Reactivation." *Infect. Immun.* **69,** (2001).

[15] Yuk, J.-M. & Jo, E.-K. "Host immune responses to mycobacterial antigens and their implications for the development of a vaccine to control tuberculosis." *Clin. Exp. Vaccine Res.* **3,** 155–67 (2014).

[16] Verma, R. K., Singh, A. K., Mohan, M., Agrawal, A. K. & Misra, A. "Inhaled therapies for tuberculosis and the relevance of activation of lung macrophages by particulate drug-delivery systems." *Ther. Deliv.* **2,** 753–768 (2011).

[17] Wildner, L. M. *et al.* "Micobactérias: Epidemiologia E Diagnóstico." *Rev. Patol. Trop.* **40,** 207–229 (2011). 55

[18] Silva, C. "Avaliação da atividade antimicrobiana de méis e água-mel." *Univ. do Algarve* (2013).

[19] Marianelli, C. *et al.* "Multiple drug-susceptibility screening in *Mycobacterium bovis*: new nucleotide polymorphisms in the embB gene among ethambutol susceptible strains." *Int. J. Infect. Dis.* **33,** 39–44 (2015).

[20] Vasconcellos, H. L. F. "Desenvolvimento de cepas de *Mycobacterium bovis* Calmette-Guérin (BCG) e *Mycobacterium smegmatis* que expressam fatores de virulência de Escherichia Coli Enteropatogênica (EPEC)." *Univ. São Paulo* (2013).

[21] Wang, R. & Marcotte, E. M. "The proteomic response of *Mycobacterium smegmatis* to anti-tuberculosis drugs suggests targeted pathways." *J. Proteome Res.* **7,** 855–865 (2008).

[22] Anes, E. *et al.* "Dynamic life and death interactions between *Mycobacterium smegmatis* and J774 macrophages." *Cell. Microbiol.* **8,** 939–960 (2006).

[23] Hett, E. C. & Rubin, E. J. "Bacterial growth and cell division: a mycobacterial perspective." *Microbiol. Mol. Biol. Rev.* **72,** 126–156 (2008).

[24] Kleinnijenhuis, J., Oosting, M., Joosten, L. a B., Netea, M. G. & Van Crevel, R. "Innate immune recognition of *Mycobacterium tuberculosis*." *Clin. Dev. Immunol.* **2011,** 405310 (2011).

[25] Vergne, I., Chua, J., Singh, S. B. & Deretic, V. "Cell biology of *Mycobacterium tuberculosis* phagosome." *Annu. Rev. Cell Dev. Biol.* **20,** 367–394 (2004).

[26] Vergne, I. *et al.* "Mechanism of phagolysosome biogenesis block by viable *Mycobacterium tuberculosis*." *Proc. Natl. Acad. Sci. U. S. A.* **102,** 4033–4038 (2005).

[27] Mishra, A. K., Driessen, N. N., Appelmelk, B. J. & Besra, G. S. "Lipoarabinomannan and related glycoconjugates: Structure, biogenesis and role in *Mycobacterium tuberculosis* physiology and host-pathogen interaction." *FEMS Microbiol. Rev.* **35,** 1126–1157 (2011).

[28] Kanwar, S. S. "Diagnostic Methods for *Mycobacterium tuberculosis* and Challenges in Its Detection in India." *Underst. Tuberc. - Glob. Exp. Innov. Approaches to Diagnosis* (2012).

[29] Piccazzo, R., Paparo, F. & Garlaschi, G. "Diagnostic Accuracy of Chest Radiography for the Diagnosis of Tuberculosis (TB) and Its Role in the Detection of Latent TB Infection: a Systematic Review." *J. Rheumatol. Suppl.* **91,** 32–40 (2014).

[30] Hickey, A. J., Misra, A. & Fourie, P. B. "Dry powder antibiotic aerosol product development: Inhaled therapy for tuberculosis." *J. Pharm. Sci.* **102,** 3900–3907 (2013).

[31] Muttil, P. *et al.* "Inhalable microparticles containing large payload of anti-tuberculosis drugs." *Eur. J. Pharm. Sci.* **32,** 140–150 (2007).

[32] Singh, M. *et al.* "Studies on toxicity of antitubercular drugs namely isoniazid, rifampicin, and pyrazinamide in an in vitro model of HepG2 cell line." *Med. Chem. Res.* **20,** 1611–1615 (2011).

[33] Whitney, J. B. & Wainberg, M. a. "Isoniazid, the frontline of resistance in *Mycobacterium tuberculosis*." *McGill J. Med.* **6,** 114–123 (2002). 56

[34] Jnawali, H. N. & Ryoo, S. "First – and Second – Line Drugs and Drug Resistance." *Tuberc. - Curr. Issues Diagnosis Manag.* 163–180 (2013).

[35] Razak, S. A., Fariq, S., Syed, F., Abdullah, J. M. & Adnan, R. "Characterization, phase solubility studies and molecular modeling of Isoniazid and its β -Cyclodextrin complexes." *J. Chem. Pharm. Res.* **6,** 291–299 (2014).

[36] Kamal, A., Azeeza, S., Shaheer Malik, M., Shaik, A. A. & Rao, M. V. "Efforts towards the development of new antitubercular agents: Potential for thiolactomycin based compounds." *J. Pharm. Pharm. Sci.* **11,** 56–80 (2008).

[37] Robertson, B. and Britton, W. "Tuberculosis." *Sci. direct* **88,** 145–7 (2008).

[38] Davies, G. R., Cerri, S. & Richeldi, L. "Rifabutin for treating pulmonary tuberculosis (Review)." *Cochrane Libr.***1,** (2010).

[39] Manuscript, A. "Experience with Rifabutin Replacing Rifampin in the Treatment of Tuberculosis." *Int J Tuberc Lung Dis. 2011* **15,** (2012).

[40] Schön, T. *et al.* "Rifampicin-resistant and rifabutin-susceptible *Mycobacterium tuberculosis* strains: A breakpoint artefact?" *J. Antimicrob. Chemother.* **68,** 2074–2077 (2013).

[41] Parikh, R., Dalwadi, S., Aboti, P. & Patel, L. "Inhaled microparticles of antitubercular antibiotic for *in vitro* and *in vivo* alveolar macrophage targeting and activation of phagocytosis." *J. Antibiot. (Tokyo).* **67,** 387–394 (2014).

[42] Marianecci, C. "Pulmonary Delivery: Innovative Approaches and Perspectives." *J. Biomater. Nanobiotechnol.* **2,** 567–575 (2011).

[43] Morais, G. G. "Otimização da terapia da tuberculose : desenvolvimento de sistemas de liberação baseados em nanotecnologia Otimização da terapia da tuberculose: desenvolvimento de sistemas de liberação baseados em nanotecnologia." *Univ. São Paulo* (2011).

[44] Grenha, A., Seijo, B. & Remuñán-López, C. "Microencapsulated chitosan nanoparticles for lung protein delivery." *Eur. J. Pharm. Sci.* **25,** 427–437 (2005).

[45] Vehring, R. "Pharmaceutical particle engineering via spray drying." *Pharm. Res.* **25,** 999–1022 (2008).

[46] Patton, J. S. & Byron, P. R. "Inhaling medicines: delivering drugs to the body through the lungs." *Nat. Rev. Drug Discov.* **6,** 67–74 (2007).

[47] Wandrey, C., Bartkowiak, A. & Harding, S. E. "Materials for Encapsulation." *Encapsulation Technol. Act. Food Ingredients Food Process.* (2010).

[48] Rodrigues, S. & Grenha, A. "Activation of Macrophages: Establishing a Role for Polysaccharides in Drug Delivery Strategies Envisaging Antibacterial Therapy." *Curr. Pharm. Des.* **21,** (2015).

[49] Sharma, J., Kaur, L., Kanuja, N., Nagpal, M. & Bala, R. "Natural Polymers-Promising Potential In Drug Delivery." *Int. J. PharmTech Res.* **5,** 684–699 (2013).

[50] Beneke, C. E., Viljoen, A. M. & Hamman, J. H. "Polymeric plant-derived excipients in drug delivery." *Molecules* **14,** 2602–2620 (2009). 57

[51] Iqbal, D. N. & Hussain, E. A. "Physiochemical and pharmaceutical properties of Guar gum derivatives." *Rep. Opin.* **2,** 77–83 (2010).

[52] Yoon, S., Chu, D. & Juneja, L. R. "Chemical and Physical Properties , Safety and Application of Partially Hydrolized Guar Gum as Dietary Fiber." *J.Clin. Biochem. Nutr.* **42,** 1–7 (2008).

[53] Mudgil, D., Barak, S. & Khatkar, B. S. "Effect of enzymatic depolymerization on physicochemical and rheological properties of guar gum." *Carbohydr. Polym.* **90,** 224–228 (2012).

[54] Munin, A. & Edwards-Lévy, F. "Encapsulation of natural polyphenolic compounds; a review." *Pharmaceutics* **3,** 793–829 (2011).

[55] Arpagaus, C., Schafroth, N. & Meuri, M. "Laboratory Scale Spray Drying of Lactose: A Review." *Inf. Bull. Büchi Switz.* 1–12 (2010).

[56] Naikwade, S. R., Bajaj, A. N., Gurav, P., Gatne, M. M. & Singh Soni, P. "Development of budesonide microparticles using spray-drying technology for pulmonary administration: design, characterization, *in vitro* evaluation, and *in vivo* efficacy study." *AAPS PharmSciTech* **10,** 993–1012 (2009).

[57] Sarraguça, M. C. *et al.* "Determination of flow properties of pharmaceutical powders by near infrared spectroscopy." *J. Pharm. Biomed. Anal.* **52,** 484–492 (2010).

[58] Liu, Y. & Nair, M. G. "An efficient and economical MTT assay for determining the antioxidant activity of plant natural product extracts and pure compounds." *J. Nat. Prod.* **73,** 1193–1195 (2010).

[59] Franzblau, S. *et al.* "Comprehensive analysis of methods used for the evaluation of compounds against *Mycobacterium tuberculosis*." *Tuberculosis* **92,** 453–488 (2012).

[60] Helguera-Repetto, A. C. *et al.* Differential macrophage response to slow- and fast-growing pathogenic mycobacteria. *Biomed Res. Int.***,** 1–10 (2014).

[61] Chanput, W. "Immunomodulating effects of food compounds: a study using the THP-1 cell line." *Wageningen Univ.* (2012).

[62] Bettencourt, P., Pires, D., Carmo, N. & Anes, E. "Application of Confocal Microscopy for Quantification of Intracellular Mycobacteria in Macrophages." *Microsc. Sci. Technol. Appl. Educ.* 614–621 (2010).

[63] Yadav, A. B. *et al.* "Microparticles induce variable levels of activation in macrophages infected with *Mycobacterium tuberculosis*." *Tuberculosis* **90,** 188–196 (2010).

[64] Jordao, L., Bleck, C. K. E., Mayorga, L., Griffiths, G. & Anes, E. "On the killing of mycobacteria by macrophages." *Cell. Microbiol.* **10,** 529–548 (2008).

[65] Rojanarat, W. *et al.* "Isoniazid proliposome powders for inhalation-preparation, characterization and cell culture studies." *Int. J. Mol. Sci.* **12,** 4414–4434 (2011).

[66] Nighute, A. B and Bhise S. B. "Preparation and Evaluation of Rifabutin Loaded Polymeric Microspheres." *Res. J. Pharm. Tech.* **2,** 371–374 (2009).

[67] Maury, M., Murphy, K., Kumar, S., Shi, L. & Lee, G. "Effects of process variables on the powder yield of spray-dried trehalose on a laboratory spray-dryer." *Eur. J. Pharm. Biopharm.* **59,** 565–573 (2005).

[68] D'Souza, S., Faraj, J. a, Giovagnoli, S. & Deluca, "P. P. Development of Risperidone PLGA Microspheres." *J. Drug Deliv.* **2014,** 11 (2014).

[69] Shah, N., Kondawar, M., Shah, R. & Shah, V. "Sustained release of spray-dried combination dry powder inhaler formulation for pulmonary delivery." *Asian J. Pharm Clin. Res.* **4,** 112–118 (2011).

[70] Javadzadeh, Y., Hamadeyazdan S., and Asnaashari S. "Recrystallization of drugs: Significance on Parmaceutical Processing." *Recrystallization* 425–447 (2012).

[71] Kim, A. I., Akers, M. J. & Nail, S. L. "The physical state of mannitol after freeze-drying: Effects of mannitol concentration, freezing rate, and a noncrystallizing cosolute." *J. Pharm. Sci.* **87,** 931–935 (1998).

[72] Hulse, W. L., Forbes, R. T., Bonner, M. C. & Getrost, M. "The characterization and comparison of spray-dried mannitol samples." *Drug Dev. Ind. Pharm.* **35,** 712–718 (2009).

[73] Padalkar, A., Shahi, S. and Thube, M. "Microparticles: An Approach for Betterment of Drug Delivery Systems." *Int. J. Pharm. Res. Dev.* **3,** 99–115 (2011).

[74] Acharya, G. *et al.* "The hydrogel template method for fabrication of homogeneous nano/microparticles." *J. Control. Release* **141,** 314–319 (2010).

[75] Kundawala, A. J., Patel, V. a, Patel, H. V & Choudhary, D. "Isoniazid loaded chitosan microspheres for pulmonary delivery : Preparation and characterization." **2,** 88–97 (2011).

[76] Alves, A. D., Cavaco, J. S. & Grenha, A. "Locust Bean Gum Microparticles as Inhalable Rifabutin Carriers for Pulmonary Tuberculosis Therapy." *Respir. Drug Deliv. Eur.* 1–6 (2015).

[77] Rodrigues, S. & Grenha, A. "K-Carrageenan microcarriers for lung delivery of antitubercular drugs." *Respir. Drug Deliv. Eur.* 1–6 (2015).

[78] EMA/CHMP/QWP. "Guideline on quality of oral modified release products." *Eur. Med. Agency* 1–16 (2014).

[79] Walters, D. V. "Lung lining liquid - The hidden depths: The 5th Nils W. Svenningsen memorial lecture." *Biology of the Neonate* **81,** 2–5 (2002).

[80] Pérez-Gil, J. "Structure of pulmonary surfactant membranes and films: The role of proteins and lipid-protein interactions." *Biochim. Biophys. Acta - Biomembr.* **1778,** 1676–1695 (2008).

[81] Rodrigues, S., Dionísio, M., López, C. R. & Grenha, A. "Biocompatibility of Chitosan Carriers with Application in Drug Delivery." *J. Funct. Biomater.* **3,** 615–641 (2012).

[82] Smith, S. M., Wunder, M. B., Norris, D. a. & Shellman, Y. G. "A simple protocol for using a LDH-Based cytotoxicity assay to assess the effects of death and growth inhibition at the same time." *PLoS One* **6,** (2011).

[83] Tsoras, A. "Development of Three-Dimensional Lung Multicellular Spheroids in Air and Liquid Interface Culture for the Evaluation of Anti-Cancer Therapeutics." *Univ. Kentucky* **11,** (2013).

[84] Möller, W., Häussinger, K., Ziegler-Heitbrock, L. & Heyder, J. "Mucociliary and long-term particle clearance in airways of patients with immotile cilia." *Respir. Res.* **7,** 10 (2006).

[85] International Organization for Standardization. "Biological Evaluation of Medical Devices Part 5: Tests for *In Vitro* Cytotoxicity." *ISO 10993–5.* (2009).

[86] Grenha, A. *et al.* "Chitosan nanoparticles are compatible with respiratory epithelial cells *in vitro*." *Eur. J. Pharm. Sci.* **31,** 73–84 (2007).

[87] Grodzki, A. C. G., Giulivi, C. & Lein, P. J. "Oxygen Tension Modulates Differentiation and Primary Macrophage Functions in the Human Monocytic THP-1 Cell Line." *PLoS One* **8,** 1–11 (2013).

[88] Guo, H., Seet, Q., Denkin, S., Parsons, L. & Zhang, Y. "Molecular characterization of isoniazid-resistant clinical isolates of *Mycobacterium tuberculosis* from the USA." *J. Med. Microbiol.* **55,** 1527–1531 (2006).

[89] Nakata, N., Kai, M. & Makino, M. "Mutation analysis of mycobacterial rpoB genes and rifampin resistance using recombinant *Mycobacterium smegmatis*." *Antimicrob. Agents Chemother.* **56,** 2008–2013 (2012).

[90] Ritz, N. *et al.* "Susceptibility of *Mycobacterium bovis* BCG vaccine strains to antituberculous antibiotics." *Antimicrob. Agents Chemother.* **53,** 316–318 (2009).

Chapter VII – Annexes

Figure 7.1 and Figure 7.2 show non-toxic formulations of PHGG polymer, PHGG and PHGG.Man in contact with A549 cells, during 3 and 24 hours of incubation.

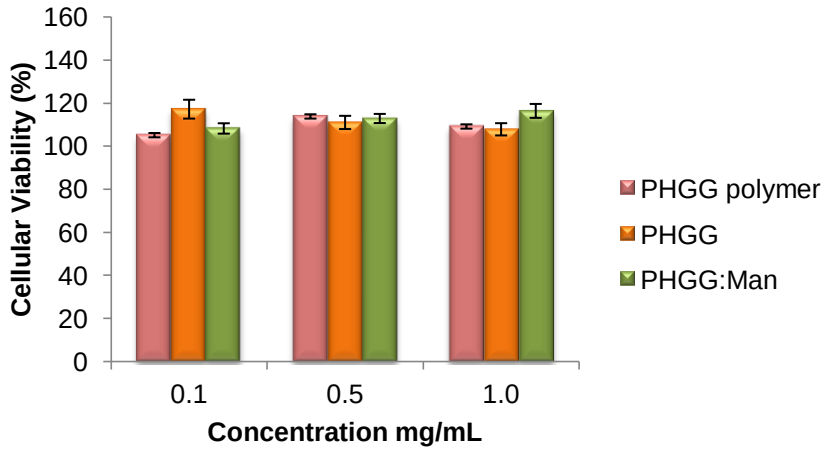

Figure 7.1 – Cell viability of A549 cells, after 3 hours of incubation with PHGG polymer, PHGG and PHGG:Man microparticles (Mean ± SEM, n = 3).

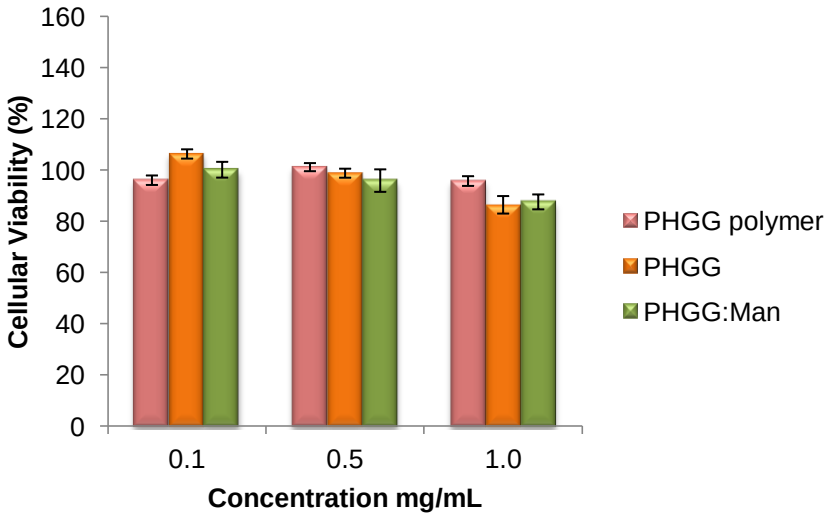

Figure 7.2 – Cell viability of A549 cells, after 24 hours of incubation with PHGG polymer, PHGG and PHGG:Man microparticles (Mean ± SEM, n = 3).

Figure 7.3 and Figure 7.4 show non-toxic formulations of PHGG polymer, PHGG and PHGG.Man in contact with Calu-3 cells, during 3 and 24 hours of incubation.

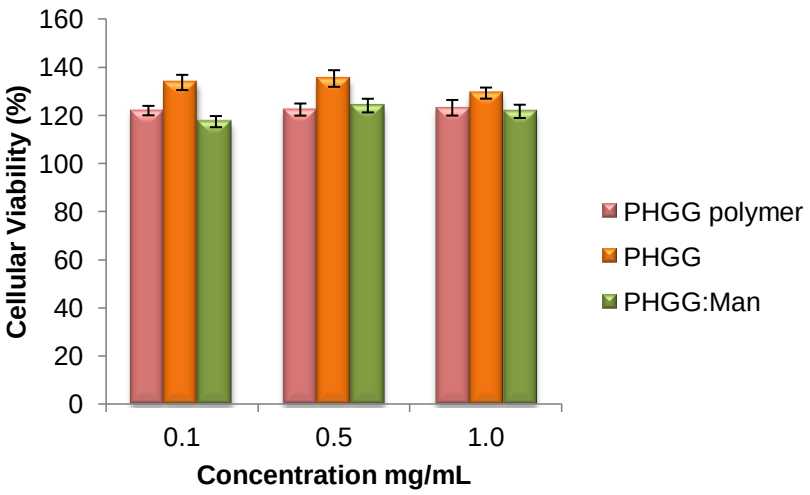

Figure 7.3 – Cell viability of Calu-3 cells, after 3 hours of incubation with PHGG polymer, PHGG and PHGG:Man microparticles (Mean ± SEM, n = 3).

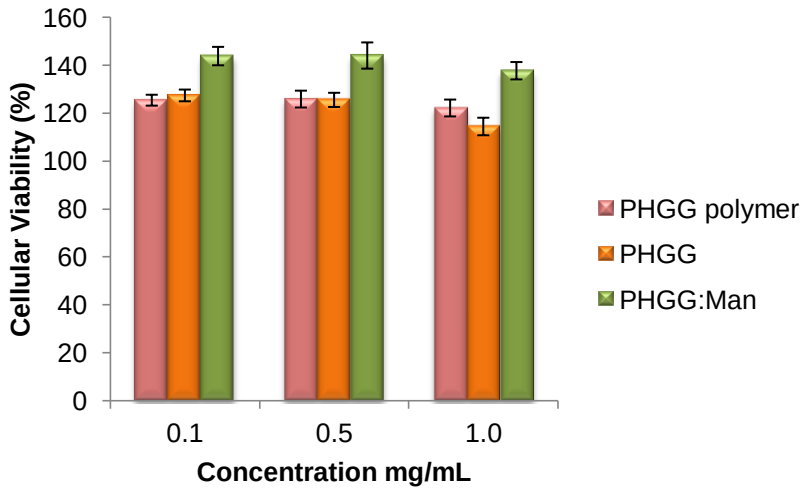

Figure 7.4 – Cell viability of Calu-3 cells, after 24 hours of incubation with PHGG polymer, PHGG and PHGG:Man microparticles (Mean ± SEM, n = 3).

Figure 7.5 show non-toxic formulations of PHGG polymer, PHGG and PHGG.Man in contact with macrophage-like cells, during 3 hours of incubation.

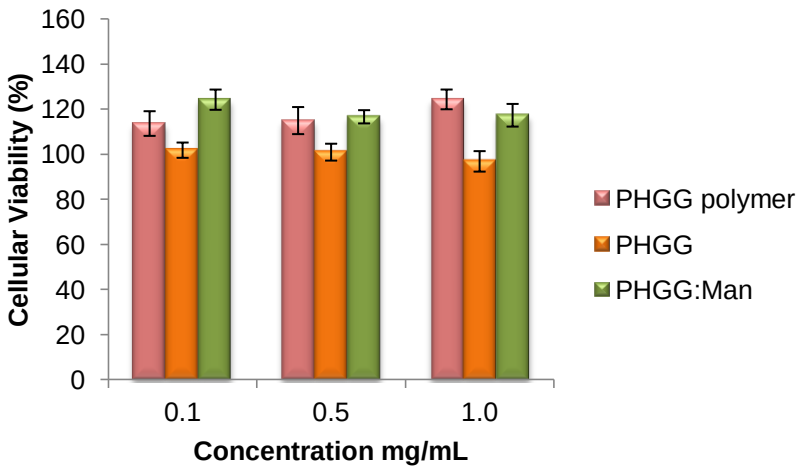

Figure 7.5 – Cell viability of macrophage-like cells, after 3 hours of incubation with PHGG polymer, PHGG and PHGG:Man microparticles (Mean ± SEM, n = 3).